

**HIGH THROUGHPUT EXPERIMENTATION WITH DESORPTION
ELECTROSPRAY IONIZATION MASS SPECTROMETRY TO GUIDE
CONTINUOUS-FLOW SYNTHESIS**

by

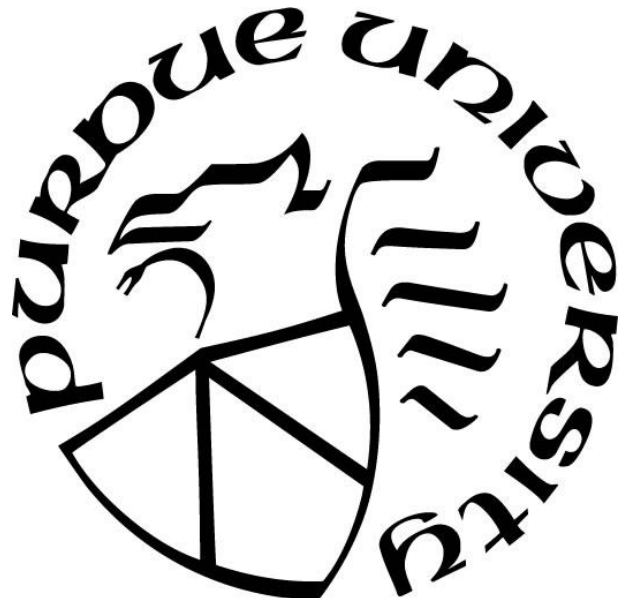
Harrison Samuel Ewan

A Dissertation

Submitted to the Faculty of Purdue University

In Partial Fulfillment of the Requirements for the degree of

Doctor of Philosophy



Department of Chemistry

West Lafayette, Indiana

December 2019

THE PURDUE UNIVERSITY GRADUATE SCHOOL
STATEMENT OF COMMITTEE APPROVAL

Dr. David H. Thompson, Chair

College of Science

Dr. R. Graham Cooks

College of Science

Dr. Christopher Uyeda

College of Science

Dr. Hilkka Kenttamaa

College of Science

Approved by:

Dr. Christine Hrycyna

I dedicate this thesis to my loving wife Stacey, who has stood by me through every challenge I have faced through the years. Her friendship, kindness and dedication made this work possible.

ACKNOWLEDGMENTS

I would like to thank my advisor Professor David Thompson for his guidance throughout my graduate career. I will be forever grateful for his instruction, encouragement, support and understanding in the time that I have known him. He was been instrumental in helping me to develop my skills as a chemist and my confidence as an independent researcher.

I would also like to acknowledge my lab mates for their continued comradery and support in the lab. They more than anyone else made the last four years a truly unforgettable experience.

Finally, I acknowledge the Defense Advanced Projects Agency, the National Science Foundation, the National Institute of Health, and the Purdue Center for Cancer Research whose grants financed this work.

TABLE OF CONTENTS

LIST OF TABLES.....	8
LIST OF FIGURES	9
LIST OF SCHEMES.....	11
ABSTRACT.....	12
CHAPTER 1. INTRODUCTION TO DESORPTION ELECTROSPRAY IONIZATION MASS SPECTROMETRY BASED HIGH THROUGHPUT EXPERIMENTATION AND MICROFLUIDIC SYNTHESIS	14
1.1 Introduction.....	14
1.2 High Throughput Experimentation with Desorption Electrospray Ionization Mass Spectrometry	15
1.2.1 Robotic Liquid Handling	15
1.2.2 DESI-MS Analysis	18
1.3 Microfluidic Synthesis.....	18
1.3.1 Introduction to Microfluidics.....	18
1.3.2 Chemtrix Reactor System	19
1.4 References.....	20
CHAPTER 2. MULTISTEP FLOW SYNTHESIS OF DIAZEPAM GUIDED BY DROPLET-ACCELERATED REACTION SCREENING WITH MECHANISTIC INSIGHTS FROM RAPID MS ANALYS.....	22
2.1 Introduction.....	22
2.2 Results and Discussion	24
2.2.1 N-Acylation Reaction Screen	24
2.2.2 Cyclization Reaction Screen.....	27
2.2.3 Continuous Diazepam Synthesis	29
2.3 Conclusions.....	30
2.4 Experimental	31
2.4.1 Reagents.....	31
2.4.2 NMR Analysis	31
2.4.3 Mass Spectrometry	31

2.4.4	Quantitative MS analysis	32
2.4.5	ESI Experiments	32
2.4.6	Leidenfrost Droplet Experiments	32
2.4.7	Microfluidic Experiments	33
2.4.8	N-(2-benzoyl-4-chlorophenyl)-2-halo-N-methylacetamide (3).....	33
2.4.9	Diazepam (4) from N-(2-benzoyl-4-chlorophenyl)-2-chloro-N-methylacetamide (3A)	
	33
2.4.10	Diazepam (4) from 5-halo-2-(methylamino)benzophenone (1).....	34
2.4.11	Batch synthesis of N-(2-benzoyl-4-chlorophenyl)-2-chloro-N-methylacetamide (3A)	
	35
2.5	Supplementary Information	35
2.6	References.....	42
CHAPTER 3.	HIGH THROUGHPUT EXPERIMENTATION USING DESI-MS TO GUIDE CONTINUOUS-FLOW SYNTHESIS FOR N-ALKYLATION REACTIONS	43
3.1	Introduction.....	43
3.2	Results and Discussion	47
3.2.1	Aniline Reactivity Screen	47
3.2.2	Expanded N-alkylation Screen	51
3.2.3	Using HTE to Scale a Reaction	54
3.2.4	Conclusions.....	55
3.3	Materials and Methods.....	57
3.3.1	General Procedure for DESI-MS Experiments.....	57
3.3.2	General Procedure for Qualitative MS Analysis	58
3.3.3	Quantitative LC/MS Analysis.....	58
3.3.4	General Procedure for Bulk Microtiter Experiments.....	59
3.3.5	General Protocol for Continuous-Flow Experiments	59
3.3.6	Continuous-Flow Degradation Experiments	59
3.3.7	Continuous-Flow Optimization Experiments	60
3.4	References.....	60

CHAPTER 4. REACTIONS OF BIO-RENEWABLE TRIACETIC ACID LACTONE PRECURSOR EVALUATED USING DESORPTION ELECTROSPRAY IONIZATION MASS SPECTROMETRY HIGH THROUGHPUT EXPERIMENTATION SYSTEM	62
4.1 Introduction.....	62
4.2 Results & Discussion	64
4.2.1 First Reaction Set.....	64
4.2.2 Expanded Reaction Set.....	67
4.2.3 Microfluidic Validation	69
4.3 Conclusions.....	73
4.4 Future Directions	73
4.4.1 TAL Acylation.....	73
4.4.2 TAL Amination	74
4.4.3 Outlook for DESI-MS HTE of Platform Molecules.....	75
4.5 Materials & Methods	76
4.5.1 General Procedure for DESI-MS Experiments.....	76
4.5.2 General Procedure for Continuous-Flow Experiments.....	76
4.5.3 General Procedure for ESI-MS Analysis.....	77
4.6 References.....	77

LIST OF TABLES

Table 2.1. Accelerations factors for the N-acylation reaction in the synthesis of Diazepam	26
Table 2.2. Microfluidic synthesis of 3A/B results, conditions and MS percent conversion.....	38
Table 2.3. Microfluidic synthesis of diazepam from intermediate 3A flow results, conditions and MS percent conversion.	39
Table 2.4. Microfluidic synthesis of diazepam from 1 flow results, in two continuous steps results, conditions, yield and MS percent conversion.	40
Table 3.1. Optimization of the reaction between cyclohexylamine and benzyl bromide. Stoichiometries are reported as ratios of amine:benzyl bromide.....	55

LIST OF FIGURES

Figure 1.1. Beckman-Coulter Biomek i7 liquid handling robot	15
Figure 1.2. Pintool dips into well plate (left), prints onto PTFE plate (right).	17
Figure 1.3. Prosolia DESI-MS stage.....	18
Figure 1.4 Chemtrix Labtrix S1Microfluidic reactor system.....	19
Figure 2.1. N-acylation screen. Synthesis of 3 in using bromoacetyl chloride – comparison of spray and flow in toluene and acetonitrile	25
Figure 2.2. Cyclization reaction screen. Synthesis of diazepam, comparing ACN(left) and toluene(right) solvents in spray, Leidenfrost and flow reactions using bromoacetyl chloride.....	26
Figure 2.3. Methylene proton 1H NMR signals of the SN2 and N-acylation product mixture....	27
Figure 2.4. Reactor schematic for continuous diazepam synthesis.	29
Figure 2.5. ¹ HNMR of [5+3B] Mixture.....	35
Figure 2.6. ¹ HNMR of [7].....	36
Figure 2.7Figure S4: ¹³ CNMR of [7].....	36
Figure 2.8. ¹ HNMR of N-(2-benzoyl-4-chlorophenyl)-2-chloro-N-methylacetamide	37
Figure 3.1. Conceptual representation of the reactor types and exchange of reactivity data between the (i) accelerated droplet reactor (ii) bulk microtiter reactor and (iii) continuous-flow reactor. Analytical tools used to monitor the reaction outcomes in each case are also shown.....	46
Figure 3.2. (A) Structures of the reaction products. Heat map representations of (B) yes/no reaction outcomes based on ion intensities in the high throughput DESI-MS experiment, (C) LC/MS quantitation of the batch experiment, and (D) LC/MS quantitation of the continuous-flow experiment. ^a Stoichiometries are reported as ratios of aniline:benzyl bromide.....	48
Figure 3.3. Heat map representations of (A) ion intensities in the high throughput DESI experiment and (B) ion intensities in the continuous-flow experiment. ^a Stoichiometries are reported as ratios of amine:benzyl bromide. *Bold outlines indicate regions of the heat map where the conditional color formatting was set.....	53
Figure 4.1. Heat map of aldol product signal intensities from aldol reactions of TAL with three substrates, three solvents, three stoichiometries, and three temperatures. Each cell is an average of 4 replicates with normalized MS intensities. Heat maps are color coded by product, separated by dark vertical lines in the table.	66

Figure 4.2. DESI-MS HTE heat map of the expanded aldol reaction set. Each cell is an average of 8 replicate reactions with normalized MS intensities. Heat maps are color coded by starting material type along the dark vertical lines in the tables. Ion intensity values are shown in the third heat map to more explicitly show the difference in substrate-based reactivity.....	68
Figure 4.3. Microfluidic reactor schematic.....	69
Figure 4.4. MS/MS spectrum of TAL.....	70
Figure 4.5. MS and MS/MS analysis of microfluidic reactions corresponding to DESI-MS HTE results.....	72
Figure 4.6. Heat map of acylation product signal intensities from aldol reactions of TAL with three substrates, three solvents, three stoichiometries and three temperatures. Each cell is an average of 4 replicates with normalized intensities. Heat maps color coded by product along the dark vertical lines.	74
Figure 4.7. Heat map of amination product signal intensities from aldol reactions of TAL with three substrates, three solvents, three stoichiometries and three temperatures. Each cell is an average of 4 replicates with normalized intensities. Heat maps color coded by product along the dark vertical lines.	75

LIST OF SCHEMES

Scheme 2.1. Proposed pathway for continuous synthesis of diazepam.....	23
Scheme 2.2. Reaction pathway to diazepam and its by-products formed during continuous flow reaction.....	29
Scheme 3.1. N-alkylation reactions executed on the DESI, batch microtiter, and continuous-flow reactor platforms.....	47
Scheme 4.1. Triacetic acid lactone (TAL)	62
Scheme 4.2. Aldol reaction of TAL and subsequent elimination.....	63
Scheme 4.3. Aldehyde starting materials used in the TAL reactivity HTE study.....	67

ABSTRACT

The present work seeks to use high throughput experimentation (HTE) to guide chemical synthesis. We demonstrate the use of an HTE system utilizing a robotic liquid handler to prepare arrays of reactions and print them onto a surface to be analyzed by desorption electrospray ionization mass spectrometry (DESI-MS) as a tool to guide reaction optimization, synthetic route selection, and reaction discovery. DESI-MS was employed as a high throughput experimentation tool to provide qualitative predictions of the outcome of a reaction, so that vast regions of chemical reactivity space may be more rapidly explored and areas of optimal efficiency identified. This work is part of a larger effort to accelerate reaction optimization to enable the rapid development of continuous-flow syntheses of small molecules in high yield. In the present iteration of this system, reactions are scaled up from these nanogram surface printed reactions to milligram scale microfluidic reactions, where more detailed analysis and further optimization may be performed. In the earliest iterations of this screening system prior to the use of DESI, the initial screening reactions were performed in electrospray (ESI) droplets and leidenfrost droplets before scaling up to microfluidic reactions which were analyzed by ESI-MS. The insights from this combined droplet and microfluidic screening/rapid ESI-MS analysis approach, helped guide the synthesis of diazepam. The system was further refined to by the use of liquid handling robots and DESI-MS analysis, greatly accelerating the overall pace of screening. In order to build confidence in this approach, however, it is necessary to establish a robust predictive connection between reactions performed under analogous DESI-MS, batch, and microfluidic reaction conditions. To achieve this goal, we first explored the potential of high throughput DESI-MS experiments to identify trends in reactivity based on chemical structure, solvent, temperature, and stoichiometry that are consistent across these platforms. While DESI-MS narrowed the scope of possibilities for reaction

selection with some parameters such as solvent, others like stoichiometry and temperature still required further optimization under continuous synthesis conditions. With our increased confidence in DESI-MS HTE, we proceeded to explore it's application to rapidly evaluate large sets of aldol reactions of triacetic acid lactone (TAL), a compound well studied for use as a bio-based platform molecule that may be converted to a range of useful commodity chemicals, agrochemicals, and advanced pharmaceutical intermediates. Our DESI-MS HTE screening technique was used to rapidly evaluate known reactions of triacetic acid lactone, in an effort to accelerate reaction discovery with platform chemicals. Our rapid experimentation system, when applied to reaction discovery in this manner, may help to shorten the time scale of platform chemical development.

CHAPTER 1. INTRODUCTION TO DESORPTION ELECTROSPRAY IONIZATION MASS SPECTROMETRY BASED HIGH THROUGHPUT EXPERIMENTATION AND MICROFLUIDIC SYNTHESIS

1.1 Introduction

The present work is a part of an effort by the Purdue Make-It collaborative team to develop an automated high throughput experimentation (HTE) system for rapid condition screening, optimization, and scale up.¹ HTE is increasingly being shown to have the potential to transform organic synthesis in much the same way as it has transformed drug discovery.²⁻¹⁰ The Purdue Make-It system utilizes multi-scale screening approach, in which nano-scale samples from robotically prepared reaction arrays are first printed onto a surface and rapidly analyzed by desorption electrospray ionization mass spectrometry (DESI-MS), in conjunction with processing and visualization software to give an easily interpreted heat map showing which reactions are viable.¹ This process gives a yes or no answer, based on a pre-determined threshold, as to the viability of thousands of reactions in a matter of hours. From these results, many otherwise time and resource consuming milli- to gram-scale reactions can be avoided in the process of route selection, scaling, and optimization. If need be, milli-scale batch reactions may be robotically prepared and analyzed via a slower but more precise technique such as electrospray MS (ESI-MS) and/or high-pressure liquid chromatography (HPLC). The results deemed successful may be next scaled up to milli-scale microfluidic reactions for further optimization. If necessary, more targeted screening may be performed with DESI-MS analysis to assist the microfluidic optimization. Reactions performed in microfluidic reactors are inherently easier to scale than the same reaction performed in batch due to superior heat and mass transfer, thus further scaling to gram and

kilogram reactions is simplified. This integrated HTE, scaling and optimization system has the potential to greatly decrease the time and material commitment when developing syntheses of valuable target molecules. The work presented in this thesis centers around the correlation between the reactions prepared in arrays and printed onto a surface for DESI-MS analysis and equivalent reactions performed in a microfluidic reactor. The experiments presented here seek to ascertain whether DESI-MS HTE provides an accurate prediction for the outcome of a microfluidic reaction. Further, as this predictive relationship becomes established, the application of DESI-MS HTE to the accelerated development of bio-renewable chemical building blocks is explored.

1.2 High Throughput Experimentation with Desorption Electrospray Ionization Mass Spectrometry

1.2.1 Robotic Liquid Handling

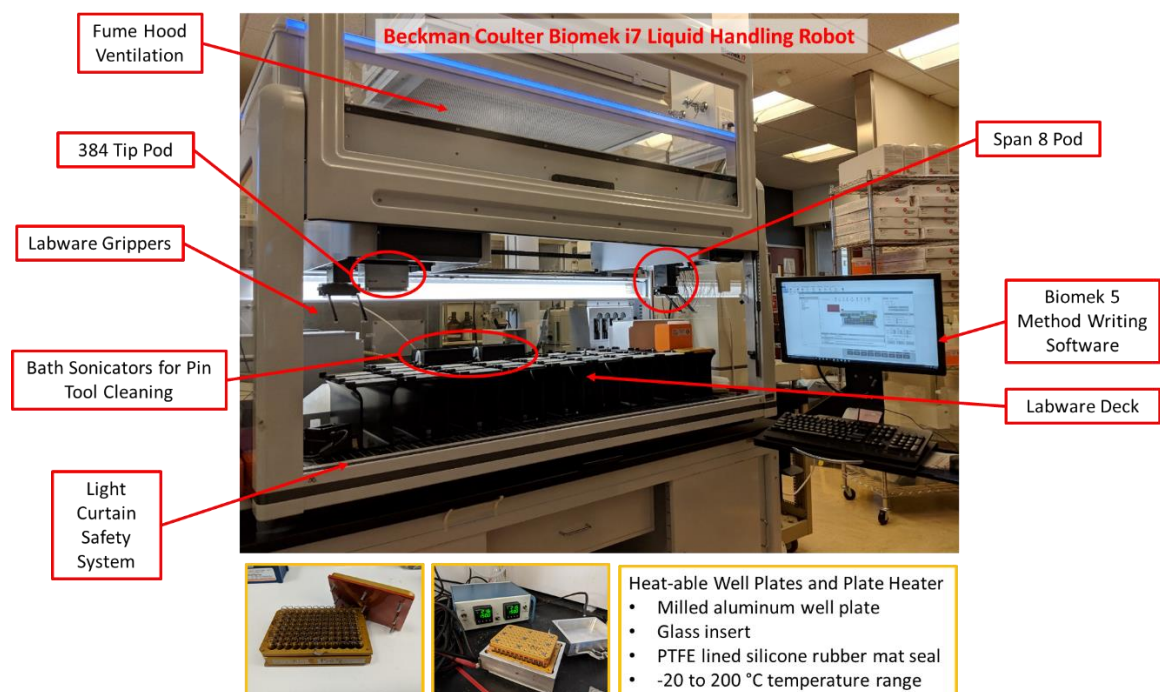


Figure 1.1. Beckman-Coulter Biomek i7 liquid handling robot.

The Darpa Make-It system utilizes the Beckman-Coulter Biomek i7 liquid handling robot to prepare reaction arrays for screening. The Biomek i7 is equipped with two independently controlled pipetting heads, one for single volume transfers of 384 pipettes at once, and another so called “span-8” head capable of pipetting 8 different volumes simultaneously. Each pipetting head is also equipped with labware grippers, capable of moving labware around the deck. The labware deck itself is laid out for standard sized well plates to fit into each position, and is protected by a “light curtain” which pauses the robot’s operation if a foreign object crosses into the deck area, keeping operators safe from the moving machinery. For the DARPA Make-It system, a fume hood ventilation system was installed to protect the operator from harmful reagent fumes. For reactions that require heating, milled aluminum 96 well plates with glass vial inserts, sealed with PTFE lined silicone rubber mats may be used to heat reactions up to reflux temperature without loss of solvent. Robotic methods for preparing reaction arrays are written with the Biomek 5 method writing software. Pipetting methods were previously optimized for the transfer of organic solvents. The Biomek 5 software is also compatible with excel, so that the operator may prepare reaction arrays on their personal computer to be incorporated into the robotic method.



Figure 1.2. Pintool dips into well plate (left), prints onto PTFE plate (right).

After reaction arrays are prepared and incubated for the desired time period, they are transferred to fresh 384 well plates (generating replicates in cases where the 96 well heatable plates are used). 50 nL samples are withdrawn from these plates using a “pin-tool” consisting of 384 slotted metal pins. The pin-tool is first dipped into the 384 source plate then printed onto a glass supported porous PTFE surface. The each reaction spots is 300 µm in diameter, allowing up to 16 spots to be printed for each well of the 384 well plate without cross-talk for a total of 6144 spots per standard surface. The pin tools are cleaned between uses via bath sonication in ethanol. After printing, the surfaces are transferred to the DESI-MS stage for analysis.

1.2.2 DESI-MS Analysis

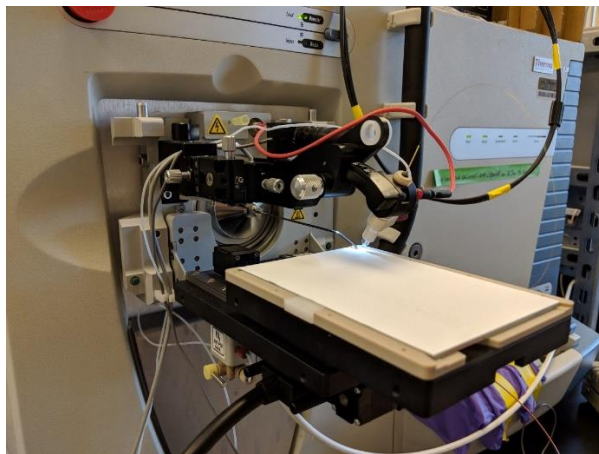


Figure 1.3. Prosolia DESI-MS stage.

DESI-MS is used to analyze the surface printed reaction array. DESI is an ambient ionization technique in which a stream of charged solvent is sprayed at the surface, causing the desorption of the surface printed material in secondary droplets that then fly into the MS detector. The surface is positioned on a movable stage, which moves underneath the spray head line after line. In this way an image in which each pixel represents a full mass spectrum is collected. By selecting a specific m/z , areas of more or less product ion abundance may be identified in order to generate a heat map of reactivity linked to the previously defined array of reactions. The raw MS data is processed by an in-house software to generate these heat maps for ease of interpretation.

1.3 Microfluidic Synthesis

1.3.1 Introduction to Microfluidics

Continuous flow synthesis has been gaining traction in recent years throughout industry and academia. The desirable qualities of continuous flow as compared to batch technologies are myriad. Continuous flow offers improved safety, lower environmental factor (E-factor),

amenability to automation, compactness, and facile reactor reconfiguration, and integration of reaction, purification, and analytics into a single compact automated system. Further, the superior mixing, improved heat and mass transfer, ease of scaling, and control over other process parameters in continuous-flow can lead to more efficient reactions and potentially even enable chemistries not possible in batch.^{6,11-17}

1.3.2 Chemtrix Reactor System

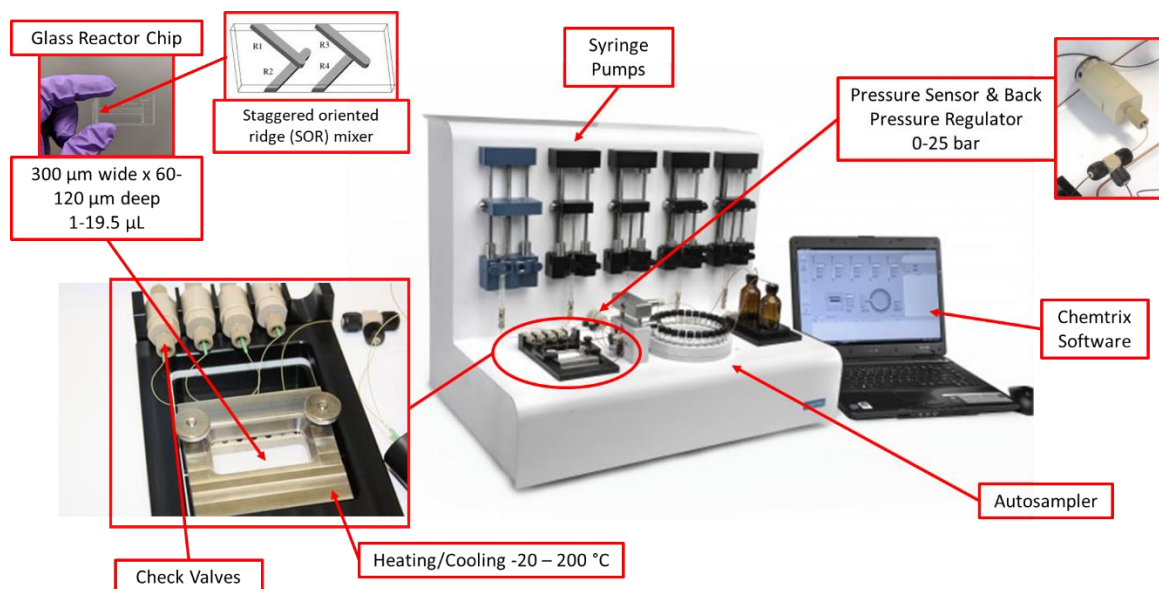


Figure 1.4 Chemtrix Labtrix S1Microfluidic reactor system.

All microfluidic reactions were carried out using the Chemtrix Labtrix S1 reactor system. This reactor uses glass reactor chips of various architectures for a broad range of chemical compatibility. In this study each glass reactor also had an incorporated “staggered oriented ridge” (SOR) mixer for thorough mass transfer. The glass reactor chip is positioned on a peltier heating stage with a temperature range of -20 to 200 °C. Each inlet to the chip is equipped with a check valve to prevent backflow into the reagent syringes, which are situated in a suite of 5 syringe pumps. A back pressure regulator (BPR) is positioned in line after the chip so reactions may be

run at high pressure and at temperatures greater than the reflux temperature of the solvent, a pressure sensor between the chip and BPR gives a constant readout of the pressure in the system. Finally, a stainless-steel needle is used to dispense reaction samples into standard HPLC vials situated on a carousel, allowing for fractional collection of reaction samples. The system is driven through the Chemtrix software, allowing for automated screening of temperature, residence time, stoichiometry, and flow rate.

1.4 References

- [1] Wleklinski, M.; Loren, B. P.; Ferreira C. R.; Jaman, Z.; Avramova, L.; Sobreira, T. J. P.; Thompson, D. H.; Cooks, R. G. *Chem. Sci.* **2018**, 9, 1647-1653
- [2] Perera, D.; Tucker, W. J.; Brahmbhatt, S.; Helal, C. J.; Chong, A.; Farrell, W.; Richardson, P.; Sach, N. W. *Science* **2018**, 359, 429-434
- [3] Mayr, L. M.; Bojanic, D., *Curr. Opin. Pharmacol.* **2009**, 9, 580-588 (2009).
- [4] Koehn, F. E., High impact technologies for natural products screening. In Natural Compounds as Drugs Volume I, Petersen, F.; Amstutz, R., Eds. Birkhäuser Basel: Basel, 2008; pp 175-210.
- [5] Janzen, W. P. *Chem. Biol.* **2014**, 21, 1162-1170
- [6] Adamo, A.; Beingessner, R. L.; Behnam, M.; Chen, J.; Jamison, T. F.; Jensen, K. F.; Monbaliu, J. C.; Myerson, A. S.; Revalor, E. M.; Snead, D. R.; Stelzer, T.; Weeranoppanat, N.; Wong, S. Y.; Zhang, P. *Science* **2016**, 352, 61-7
- [7] Zhang, P.; Weeranoppanat, N.; Thomas, D. A.; Tahara, K.; Stelzer, T.; Russel, M. G.; O'Mahony, M.; Myerson, A. S.; Lin, H.; Kelly, L. P.; Jensen, K. F.; Jamison, T. F.; Dai, C.; Cui, Y.; Briggs, N.; Beingessner, R. L.; Adamo, A. *Chem. Eur. J.* **2018**, 24, 2776-2784
- [8] Fitzpatrick, D. E.; Battilocchio, C.; Ley, S. V. *ACS Cent. Sci.* **2016**, 2, 131-138
- [9] Mascia, S.; Heider, P. L.; Zhang, H.; Lakerveld, R.; Benyahia, B.; Barton, P. I.; Braatz, R. D.; Cooney, C. L.; Evans, J. M. B.; Jamison, T. F.; Jensen, K. F.; Myerson, A. S.; Trout, B. L. *Angew. Chem. Int. Ed.* **2013**, 52, 12359-63
- [10] Reizman, B. J.; Wang, Y; Buchwald, S. L.; Jensen, K. F. *React. Chem. Eng.* **2016**, 1, 658-666

- [11] Bédard, A.; Longstreet, A. R.; Britton, J.; Wang, Y.; Moriguchi, H.; Hicklin, R. W.; Green, W. H.; Jamison, T. F. *Bioor. Med. Chem.* <http://dx.doi.org/10.1016/j.bmc.2017.02.002>
- [12] Baumann, M.; Baxendale, I. R. *Beilstein J. Org. Chem.* **2015**, 11, 1194-1219
- [13] Malet-Sanz, L.; Susanne, F. *J. Med. Chem.* **2012**, 55, 4062-4098
- [14] McQuade, D. T.; Seeberger, P.H. *J. Org. Chem.* **2013**, 78, 6384-6389
- [15] Ewan, H. S.; Iyer, K.; Hyun, S.; Wleklinski, M.; Cooks, R. G.; Thompson, D. H. *Org. Process Res. Dev.*, **2017**, 21, 1566-1570
- [16] Loren, B. P.; Wleklinski, M.; Koswara, A.; Yammie, K.; Hu, Y.; Nagy, Z. K.; Thompson, D. H.; Cooks, R. G. *Chem. Sci.* 2017, 8, 4363-4370
- [17] Falcone, C. E.; Jaman, Z.; Wleklinski, M.; Koswara, A.; Thompson, D. H.; Cooks, R. G. *Analyst*, **2017**, 142, 2836-2845

CHAPTER 2. MULTISTEP FLOW SYNTHESIS OF DIAZEPAM GUIDED BY DROPLET-ACCELERATED REACTION SCREENING WITH MECHANISTIC INSIGHTS FROM RAPID MS ANALYS

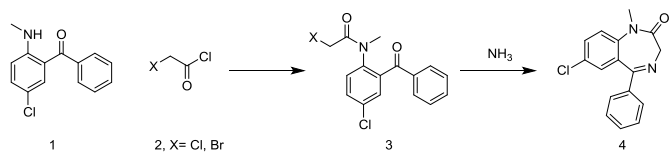
This chapter was originally published in Organic Process Research & Development: Ewan, H. S.; Iyer, K.; Hyun, S.; Wleklinski, M.; Cooks, R. G.; Thompson D. H. *Org. Process Res. Dev.* **2017**, 21, 1566-1570

2.1 Introduction

The potential for the efficient synthesis of active pharmaceutical ingredients (APIs) through continuous flow chemistry continues to draw interest from a broad range of disciplines throughout academia and industry.^{1,2,3,4,5} Mass spectrometry (MS) has proven to be a useful tool in reaction monitoring as it allows monitoring of the kinetics and outcome of a reaction.⁶ MS also helps in identifying reactive intermediates, and hence in understanding the mechanistic details of a chemical reaction.⁷ Additionally, MS can be used to study chemical reactions in droplets.⁸ Previous studies have shown that most chemical reactions are accelerated in microdroplets formed by electrospray ionization (ESI) relative to the corresponding bulk reactions.^{9,10} This acceleration is due, in part, to solvent evaporation and its effect on reagent concentration at the interface.¹¹ This rapid method of reaction screening can be useful in guiding microfluidic reactions and in scale up. An alternative way of generating microdroplets for studying chemical reactions is by employing the Leidenfrost effect. This effect occurs when a solution is dropped onto a heated surface such as a glass petri dish which is held at a temperature higher than the boiling point of the solvent used. As the droplet approaches the heated surface, the solvent begins to evaporate and a layer of insulating vapor is formed around the droplet. This prevents rapid evaporation of the solvent and causes the droplet to levitate.¹² Although the droplets that are formed by this technique are larger

than ESI droplets, they have some of the same properties, therefore reactions in these droplets can also be a useful tool in guiding microfluidic transformations.

In the present study, we use the synthesis of diazepam (Scheme 2.1) as a model system to showcase how the droplet screening demonstrated by Wleklinski et.al.¹³ guided the continuous synthesis of diazepam. Since a key step in this pathway involves N-acylation, these observations may have a more general bearing on N-acylation reactions in the synthesis of common bioactive molecules.¹⁴ Although microdroplet conditions do not always directly translate into microfluidic scale conditions, this method can serve as a rapid yes/no prediction tool for the likelihood of a productive microfluidic reaction. Flow chemistry systems, coupled with on-line monitoring by ESI-MS, enable rapid screening of reaction conditions with real-time feedback. Not only does this allow for facile and efficient synthesis of APIs, but it also brings an opportunity for new insights into reaction pathways and byproduct formation. Diazepam may be obtained in two synthetic steps, starting from the N-acylation reaction of 5-chloro-2-(methylamino)benzophenone 1 with 2-haloacetyl chloride 2 giving amide 3. Subsequent treatment with ammonia then results in cyclization, giving diazepam 4 (Scheme 2.1). For each reaction screened in droplets or examined in flow reaction systems, the outcome was immediately ascertained by ESI-MS analysis.



Scheme 2.1. Proposed pathway for continuous synthesis of diazepam.

2.2 Results and Discussion

2.2.1 N-Acylation Reaction Screen

Reaction screening began with examination of the N-acylation step in ESI droplets, Leidenfrost droplets, bulk, and flow reaction systems. Initial ESI spray (offline) reaction screening across several solvents [dimethylacetamide (DMA), tetrahydrofuran(THF), dimethylformamide(DMF), acetonitrile(ACN), N-methylpyrrolidone(NMP) and toluene] revealed significant acceleration in ACN (~35x) and toluene (~100x) relative to a 30-minute screen of the reaction in bulk at the same initial concentrations (Figure 2.1, Table 2.1). Although the spray experiment was performed in different solvents, the final extraction before analysis was done in ACN for all experiments.

Screening of flow reaction conditions for the first step also began with a solvent screen. NMP and DMF performed poorly giving limited conversion and significant impurities. N-acylation occurred rapidly and with good conversion in toluene, whereas in ACN, the formation of side products (5, 7) arising from the SN₂ reaction pathway were observed (Figure 2.1).¹³ In addition to solvents, temperatures and residence times were varied (Table 2.3). With increasing temperature, in most cases, conversion was poorer due to increasingly prevalent side reactions. By exchanging chloroacetyl chloride for bromoacetyl chloride, we obtained evidence of an alternative reaction pathway (previously reported by Wleklinski et al.).¹³ The molecular weight of the expected product of this N-acylation reaction using bromoacetyl bromide is 367; however, we saw an additional peak at m/z 322. This corresponds to a loss of bromine rather than chlorine, as expected from N-acylation. A mixture of the SN₂ and N-acylation products (from the flow experiment) was isolated by column chromatography, and though they could not readily be separated from one another, NMR analysis showed two distinct sets of peaks at 3.7 and 3.9 ppm,

corresponding to the methylene protons of the N-acylation and SN₂ products, respectively (Figure 2.3, Figure 2.4). Guided by these observations regarding the mechanism of the reaction where one solvent favored the more desired pathway and products, we determined that toluene was the optimal solvent for the continuous synthesis of diazepam.

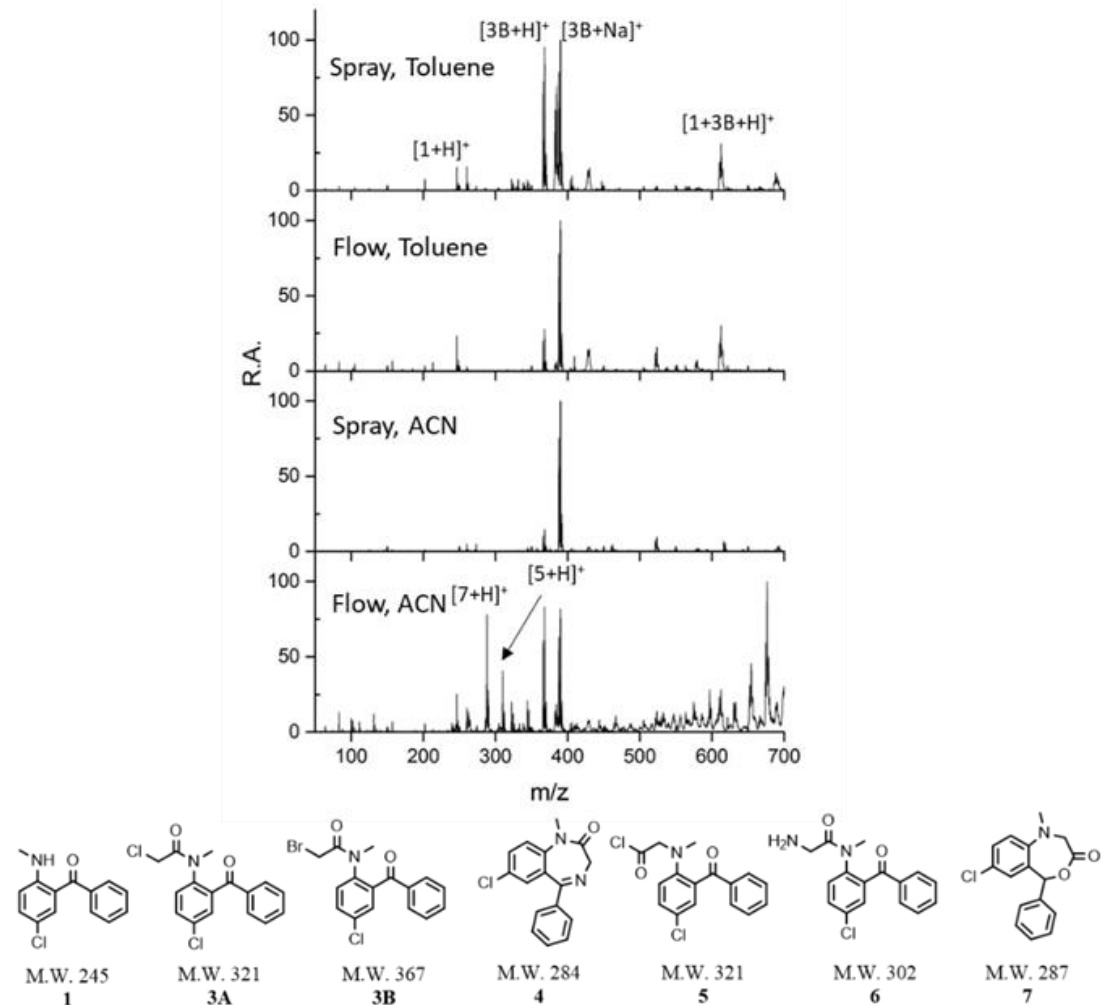


Figure 2.1. N-acylation screen. Synthesis of 3 in using bromoacetyl chloride – comparison of spray and flow in toluene and acetonitrile

Table 2.1. Accelerations factors for the N-acylation reaction in the synthesis of Diazepam

Solvent	Starting Material	Acceleration factor [#]	
		ESI Spray	Leidenfrost
Acetonitrile	Chloroacetyl chloride	35	25
	Bromoacetyl chloride	29	24
Toluene	Chloroacetyl chloride	97	14
	Bromoacetyl chloride	38	34

Acceleration factors reported in Table 2.1 are apparent acceleration factors given by the ratio of the mass spectrometry signals for the products relative to the starting materials (i.e. the conversion ratio) in the micro droplets relative to the bulk. This is not the same as the ratio of the rate constants for the two media.

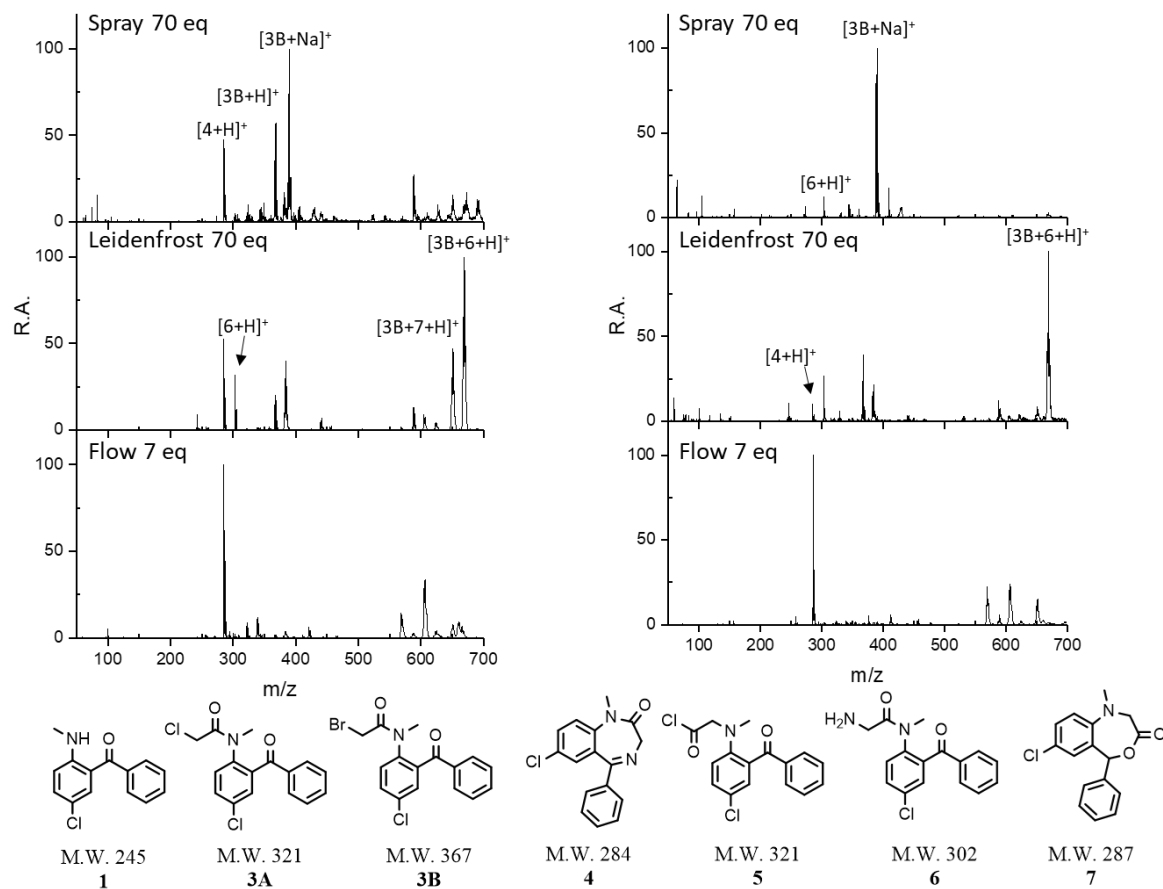


Figure 2.2. Cyclization reaction screen. Synthesis of diazepam, comparing ACN(left) and toluene(right) solvents in spray, Leidenfrost and flow reactions using bromoacetyl chloride.

In addition to this SN2 product, we also observed a peak at m/z 288 in our flow experiments, consistent with ring closure to produce a 7-membered lactone. We propose that this m/z 288 compound (mol.wt. 287) is a result of an initial SN2 reaction, followed by nucleophilic attack by the carbonyl on the acyl chloride to form the 7-membered ring. ¹H and ¹³CNMR analysis confirmed this proposed structure (Figures 2.3 and 2.4, respectively). This result suggests that the selection of reaction solvent and halide can be used to exert control over the reaction outcome in a microfluidic system. It is noteworthy that these alternative outcomes were observed in the microfluidic experiment, but were absent in the corresponding droplet experiments. We believe that this is due to the high temperature and pressure conditions accessible in microfluidic reactions, but absent in droplet reactions, making alternative reaction pathways with higher energy requirements more likely.

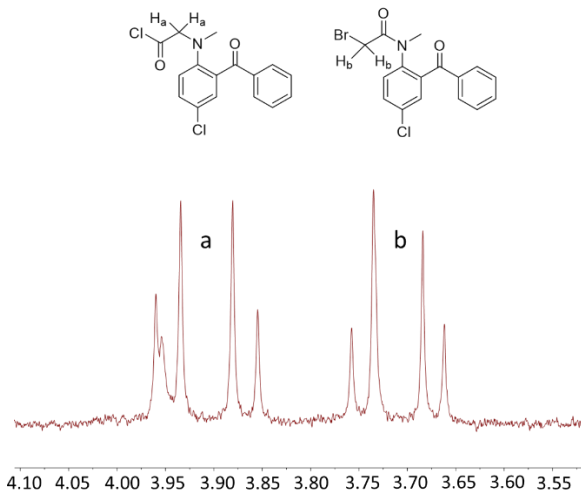


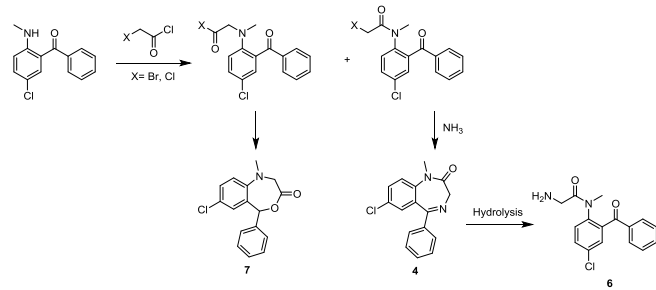
Figure 2.3. Methylene proton ¹H NMR signals of the SN2 and N-acylation product mixture.

2.2.2 Cyclization Reaction Screen

Previous screening of the cyclization reaction space revealed that a greater concentration of ammonia was required to form diazepam in Leidenfrost droplets (Figure 2.2). Reaction

acceleration was observed in these droplet reactions and they corroborated the microfluidic screen. A microfluidic screen of the second step from the N-acylation product 3A, prepared previously, was carried out prior to attempting both steps in continuous flow. The solvent screen was limited by the low solubility of the chloro version of the intermediate (previously prepared in batch). For each solvent, varying temperatures and residence times were screened. The material was insoluble at a target concentration of 250 μ M in ACN and toluene, but dissolved well in NMP at this concentration. Fortunately, a good conversion to diazepam was observed in NMP (Table 2.3). Another interesting observation when studying this step was the appearance of a peak at m/z 303. We anticipated that this might represent a substitution of nitrogen at the methyl position. Due to the appearance of this peak in the MS at lower temperatures and residence times, and disappearance at higher temperatures, we also believed that it might be an intermediate in the diazepam synthesis. LC-MS analysis revealed that despite the previous MS observation, the quantity of this m/z 303 material remained relatively constant throughout the temperature and residence time screen, even as the quantity of diazepam steadily increased. This could be in part due to high ionization efficiency of the m/z 303 material drowning out the signal from other compounds present in the reaction mixture. This m/z 303 material (6) is believed to be a previously reported hydrolysis product of diazepam.¹⁵

2.2.3 Continuous Diazepam Synthesis



Scheme 2.2. Reaction pathway to diazepam and its by-products formed during continuous flow reaction.

Based on these observations, we were able to develop a more complete understanding of the possible outcomes of each synthetic step of our synthetic route to diazepam. These possible reaction pathways are summarized in Scheme 2. Guided by this knowledge from our screening, we next attempted to optimize the synthesis of diazepam in two continuous steps. We used a two-chip reactor system to allow for finer control of temperature and residence time in each chip. The first chip combined 5-chloro-2-(methylamino)benzophenone and haloacetyl chloride in a 1:2 ratio, respectively (Figure 2.4, R1 and R2), before dilution of the resultant N-acylation product mixture (R3) with methanol and subsequent addition of ammonia/methanol (R4) in a 7-fold excess in the second chip.

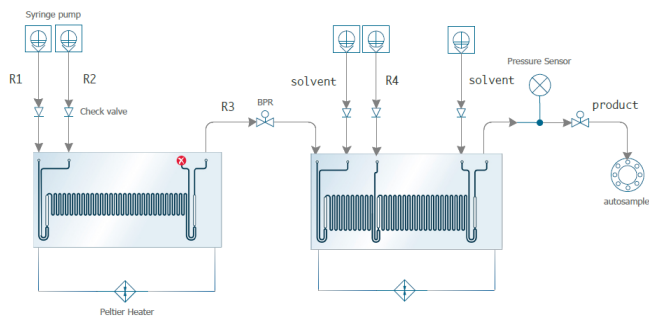


Figure 2.4. Reactor schematic for continuous diazepam synthesis.

Solvent screening was again limited by solubility, particularly upon addition of ammonia/methanol in the second step. In order to alleviate this problem, a dilution step after the first reaction step was incorporated to improve solubility. Good solubility was achieved using toluene for the first step and diluting 1:4 with methanol or NMP. Use of ACN in the first step and for dilution was also effective. As in the previous flow reaction screens, we varied temperature and residence time, as well as the selection of bromo- vs. chloroacetyl chloride (Table 2.4). The results of this screen seemed to corroborate our previous observations, with bromoacetyl chloride resulting in some SN₂ product, particularly in ACN. Furthermore, the overall conversion from the intermediate to diazepam was higher when bromoacetyl chloride was used.

Yields for each reaction were determined using a quantitative ESI-MS/MS method. The optimum result was achieved using bromoacetyl chloride in the toluene/methanol solvent system, which yielded diazepam in 100% yield, based on our ESI-MS quantitation method. This was also the optimal solvent system in Leidenfrost and spray microdroplets.

2.3 Conclusions

This study, using the diazepam synthesis as a model reaction, demonstrates the ability of MS analysis and droplet reactions to guide microfluidic synthesis. MS can be used not only as an analytical tool, but can also serve as a quick way to predict reactivity and guide microscale synthesis. The use of spray and Leidenfrost droplet reactions as a screening step to guide the larger scale microfluidic screening proved a useful tool in predicting the overall outcome of a reaction. While some nuances observed in flow reactions were not observed in droplet experiments, these experiments still consistently provided a yes/no indication of the viability of a reaction. Further, we have demonstrated the continuous synthesis of diazepam in two steps in a microfluidic flow

reactor. Our synthesis features the use of a mixed solvent system, as well as two microfluidic chips in sequence, allowing for optimized temperature control at each step. Additionally, we have identified previously unknown reaction pathways. These results showcase the possibility for microfluidic synthesis coupled with rapid ESI-MS analysis to identify previously unknown reaction pathways and optimize continuous synthesis of APIs.

2.4 Experimental

2.4.1 Reagents

Reagents were purchased from Sigma-Aldrich and used without further purification.

2.4.2 NMR Analysis

NMR Samples were prepared by micro-scale SiO₂ column chromatography. Samples were analyzed using a Bruker AV-III-500-HD NMR spectrometer.

2.4.3 Mass Spectrometry

Mass spectral analysis of reaction products was performed using an LTQ ion trap mass spectrometer (Thermo Fisher Scientific, San Jose, CA) with nanoESI ionization. All product samples (spray, Leidenfrost, or flow reactions) were diluted 1:100 into ACN before analysis, unless otherwise noted. The distance between the tip of the spray emitter and ion transfer capillary to the MS was kept constant at ca. 1 mm. Experiments were performed using borosilicate glass pulled to a ca. 1–3 μm aperture. A spray voltage of either positive or negative 2.0 kV was used for all analyses. Positive-ion mode was used for all chemical analyses, unless otherwise noted. Product

ion (MS/MS) spectra were recorded using collision-induced dissociation (CID) with a normalized collision energy of 25 (manufacturer's unit).

2.4.4 Quantitative MS analysis

An MS based calibration was made from mixtures of 0M, 1x10⁻⁷M, 1x10⁻⁶M, 2.5x10⁻⁶M, and 8x10⁻⁶M Diazepam with 3.88x10⁻⁶M Diazepam-D3. Each point was measured with nESI in triplicate and the calibration is based on the Diazepam to Diazepam-D3 ratio. Crude reaction samples were quantified by first diluting an appropriate amount (x10,000 typically) and then adding the same amount of internal standard. Each crude sample was diluted in duplicate and analyzed by nESI.

2.4.5 ESI Experiments

These experiments were performed by spraying the reaction mixture directly onto glass wool and then extracting the sprayed residue with ACN. The extract was diluted 1:100 then analyzed by MS. A homebuilt electrospray ionization source was used. Reagents 1 and 2 were premixed at concentrations of 100 mM and 200 mM, respectively, and loaded into a syringe. Offline spray was carried out at a flow rate of 10 µL/min, 100 psi N₂ sheath gas and 5 kV voltage. The total spray time was 10 minutes. After MS analysis, the washed material was drawn back into the syringe and mixed with ammonia in methanol and then electrosprayed in order to synthesize diazepam.

2.4.6 Leidenfrost Droplet Experiments

This experiment was carried out on a hot plate with a heat setting of 540 °C (although the droplet temperature was much lower). Reagents 1 and 2 were premixed and loaded into a Pasteur

pipette. The reaction mixture was then dropped onto a glass Petri dish that was placed on the hot plate. The reaction mixture was added in aliquots over a time period of about 2 minutes. After 2 minutes, the mixture was collected from the surface using a Pasteur pipette and then analyzed by MS after diluting 1:2.

2.4.7 Microfluidic Experiments

All microfluidic reactions were carried out using a Chemtrix Labtrix S1 system, equipped with 3223 or 3224 reactor chips.

2.4.8 N-(2-benzoyl-4-chlorophenyl)-2-halo-N-methylacetamide (3)

Solutions (100 mM) of 5-halo-2-(methylamino)benzophenone (1 equiv.) and of haloacetyl chloride (1 equiv.) in toluene, ACN, DMF, or NMP were prepared. In the DMF reaction screen, 500 mM solutions were used; in the NMP reaction screens, 250 mM solutions of benzophenone and 500 mM (2 equiv.) chloroacetyl chloride were used. A syringe was loaded with each of these two solutions, and positioned on the first two inlets of a 10 μ L Labtrix 3223 chip. A third syringe was loaded with toluene and positioned on the third port of the same chip as a diluent. The reaction was flowed with 30, 60, and 180 second residence times at temperatures of 50, 100, and 150°C. Samples were collected and immediately analyzed by ESI-MS (1 μ L of each sample was diluted with 99 μ L of ACN, then loaded into a glass electrospray tip for analysis). Samples were saved and stored at -20°C.

2.4.9 Diazepam (4) from N-(2-benzoyl-4-chlorophenyl)-2-chloro-N-methylacetamide (3A)

A 250 mM solution of N-(2-benzoyl-4-chlorophenyl)-2-chloro-N-methylacetamide (1 equiv.) as prepared. Syringes were loaded with the prepared solution and with 7 N ammonia in

methanol (7 equiv.) and positioned on the first two inlets of a 10 μ L Labtrix 3223 chip. A third syringe was loaded with NMP and positioned on the third port of the same chip as a diluent. The reaction was flowed with 30, 60, and 180 second residence times at temperatures of 50, 100, and 150°C. Samples were collected and immediately analyzed by ESI-MS (1 μ L of each sample was diluted with 99 μ L of ACN, then loaded into a glass electrospray tip for analysis). Samples were saved and stored at -20°C.

2.4.10 Diazepam (4) from 5-halo-2-(methylamino)benzophenone (1)

Solutions (100 mM) of 5-halo-2-(methylamino)benzophenone (1 equiv.) and 200 mM haloacetyl chloride (2 equiv.) in toluene or ACN were prepared. Syringes were loaded with the prepared solutions and with 7 N ammonia in methanol (7 equiv.). The syringes containing 5-halo-2-(methylamino)-benzophenone and haloacetyl chloride were positioned on the first two inlets of a 10 μ L Labtrix 3223 chip. The mixture was flowed into a second 15 μ L Labtrix 3224 chip through the first inlet. A syringe containing toluene, NMP, or ACN was positioned at the second inlet of the 3224 chip to dilute the reaction by 1:4. The syringe containing 7 N ammonia in methanol was positioned at the third inlet of the 3224 chip. A final syringe containing toluene, NMP or ACN was positioned at the final inlet of the 3224 chip, flowing at a low flow rate of solvent to help avoid fouling at the outlet. The reaction was flowed with residence times of 1+0.32 s and 2+0.62 s (chip 1 + chip 2) and temperatures of 75 °C in chip 1 and 100, 110, 120, or 140 °C in the second chip. Samples were collected and immediately analyzed by ESI-MS (1 μ L of each sample was diluted with 99 μ L of ACN, then loaded into a glass electrospray tip for analysis). Samples were saved and stored at -20°C.

2.4.11 Batch synthesis of N-(2-benzoyl-4-chlorophenyl)-2-chloro-N-methylacetamide (3A)

Chloroacetyl chloride (0.39 mL, 4.9 mmol, 1 EQ) was added to a solution of 5-chloro-2-(methylamino)benzophenone (1.2 g, 4.9 mmol) in 100 mL NMP (50 mM). The reaction was heated to 90°C for 40 min. The solution was then concentrated in vacuo and the product was isolated via SiO₂ column chromatography in 68% yield. The structure was confirmed by ¹HNMR (Figure 2.7).

2.5 Supplementary Information

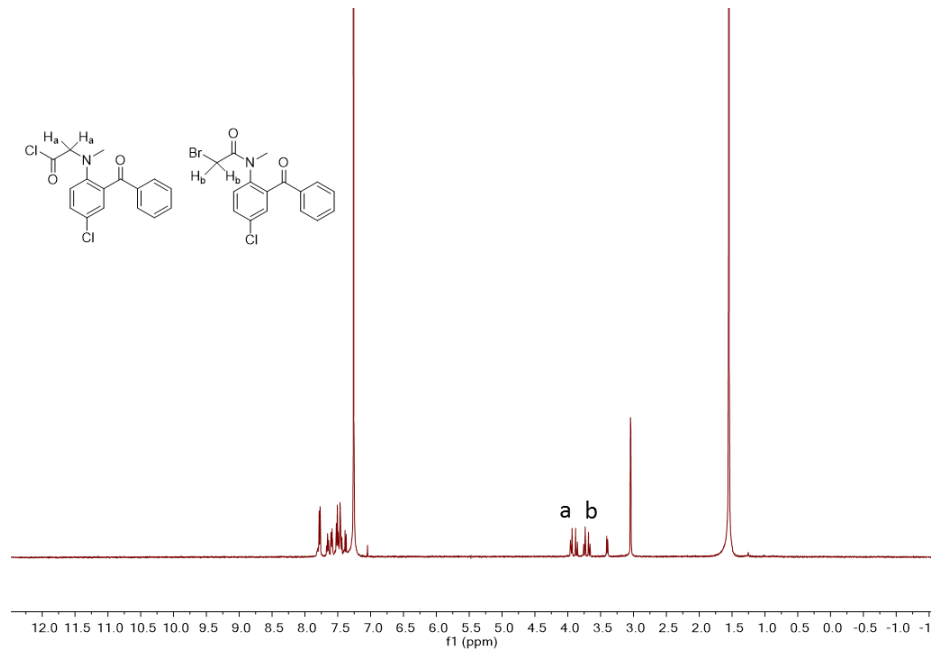


Figure 2.5. ¹HNMR of [5+3B] Mixture.

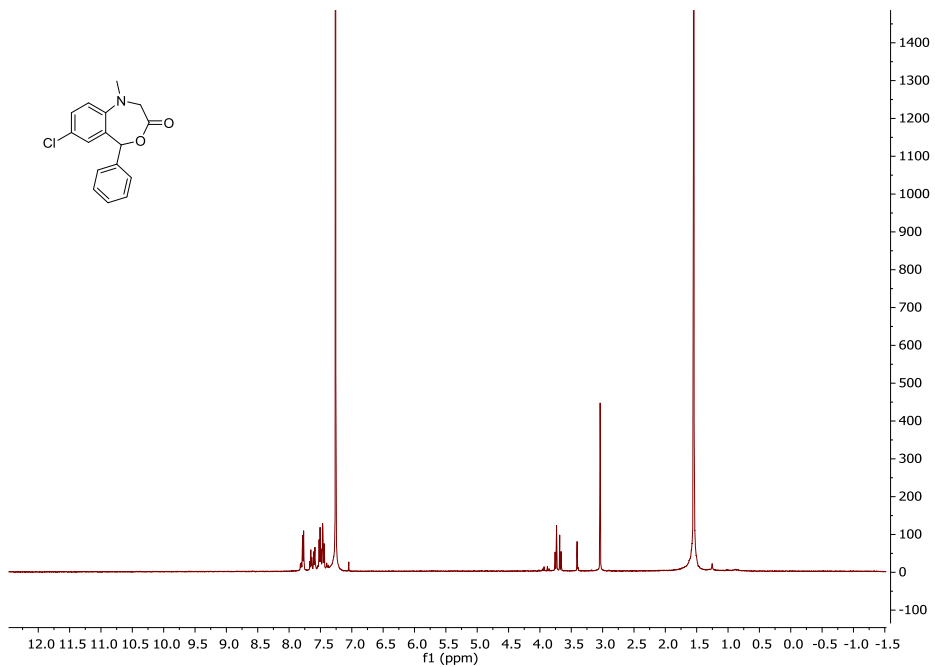


Figure 2.6. ^1H NMR of [7].

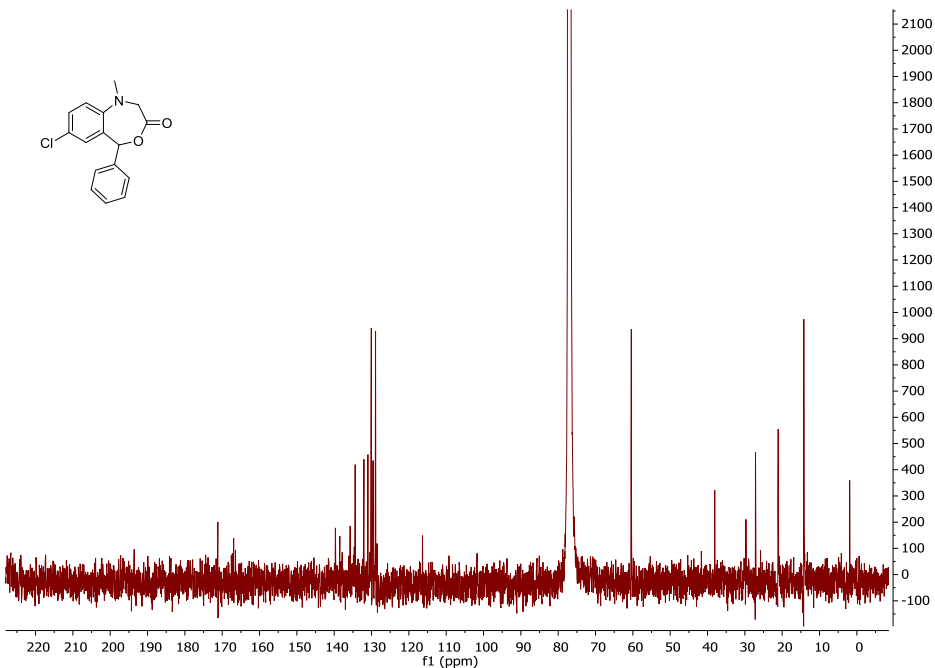


Figure 2.7Figure S4: ^{13}C NMR of [7].

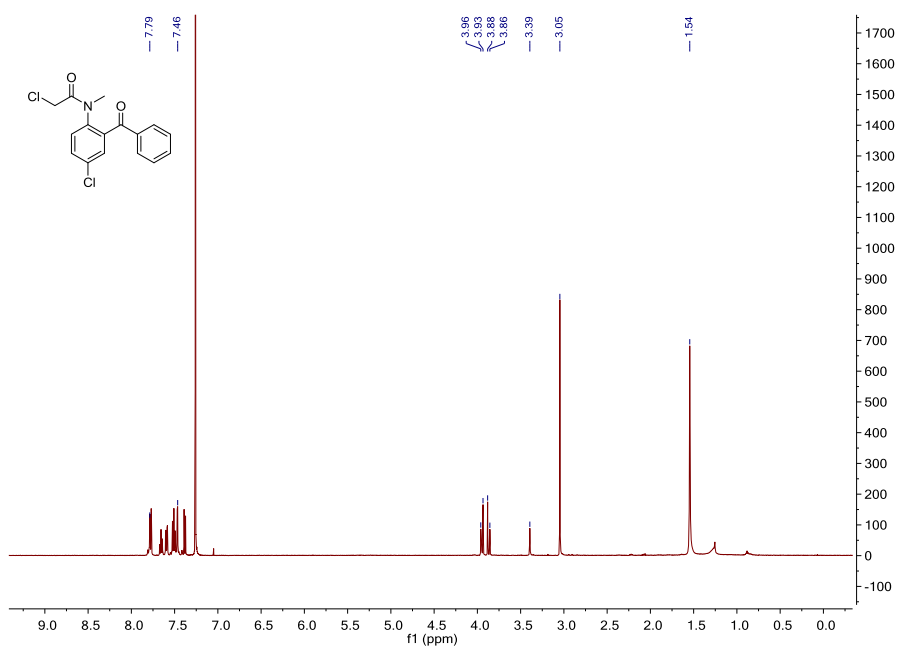


Figure 2.8. ^1H NMR of N-(2-benzoyl-4-chlorophenyl)-2-chloro-N-methylacetamide

Table 2.2. Microfluidic synthesis of **3A/B** results, conditions and MS percent conversion.

#	SOLVENT	X	T (°C)	TR (S)	% [1]	% [3A/B]	% [5]	% [6]
1	ACN	Br	50	30	2	80	5	19
2	ACN	Br	50	60	10	65	5	19
3	ACN	Br	50	180	3	16	3	79
4	ACN	Br	100	180	1	26	7	67
5	ACN	Br	100	60	14	21	6	59
6	ACN	Br	100	30	14	28	5	54
7	ACN	Br	150	30	7	24	4	65
8	ACN	Br	150	60	6	17	4	73
9	ACN	Br	150	180	9	13	3	74
10	ACN	Cl	50	30	0	100	0	0
11	ACN	Cl	50	60	0	100	0	0
12	ACN	Cl	50	180	0	100	0	0
13	ACN	Cl	100	180	1	99	0	0
14	ACN	Cl	100	60	1	99	0	0
15	ACN	Cl	100	30	0	100	0	0
16	ACN	Cl	150	30	0	100	0	0
17	ACN	Cl	150	60	0	100	0	0
18	ACN	Cl	150	180	0	100	0	0
19	Toluene	Br	50	30	29	70	0	1
20	Toluene	Br	50	60	14	85	1	1
21	Toluene	Br	50	180	32	65	1	10
22	Toluene	Br	100	180	21	74	2	18
23	Toluene	Br	100	60	32	65	2	3
24	Toluene	Br	100	30	31	67	1	1
25	Toluene	Br	150	30	25	74	1	1
26	Toluene	Br	150	60	36	63	1	2
27	Toluene	Br	150	180	31	66	2	10
28	Toluene	Cl	50	30	2	98	0	0
29	Toluene	Cl	50	60	1	99	0	0
30	Toluene	Cl	50	180	6	94	0	0
31	Toluene	Cl	100	180	5	95	0	0
32	Toluene	Cl	100	60	12	88	0	0
33	Toluene	Cl	100	30	18	82	0	0
34	Toluene	Cl	150	30	16	84	0	0
35	Toluene	Cl	150	60	11	89	0	0
36	Toluene	Cl	150	180	10	90	0	0

Table 2.3. Microfluidic synthesis of diazepam from intermediate **3A** flow results, conditions and MS percent conversion.

#	SOLVENT	X	T (°C)	TR (S)	% [3A]	% [4]	% [6]
1	NMP	Cl	50	30	34	1	65
2	NMP	Cl	50	60	37	1	62
3	NMP	Cl	100	30	39	1	60
4	NMP	Cl	100	60	33	2	65
5	NMP	Cl	150	30	29	17	54
6	NMP	Cl	150	60	15	51	34

Table 2.4. Microfluidic synthesis of diazepam from **1** flow results, in two continuous steps results, conditions, yield and MS percent conversion.

#	YIELD (%)	SOLVENT	X	T _{CHIP1} (°C)	T _{CHIP2} (°C)	T _R (CHIP1+2)	(MIN, [1])	% [1]	% [3A/B]	% [4]	% [5]	% [7]	% [6]
1	7	Toluene/ MeOH	Br	75	150	1+0.32	6	44	42	3	1	4	
2	2	Toluene /MeOH	Br	75	140	1+0.32	65	10	17	6	1	1	
3	16	Toluene /MeOH	Br	75	100	1+0.32	0	62	32	1	2	3	
4	18	Toluene /MeOH	Br	75	110	1+0.32	0	53	40	2	3	2	
5	22	Toluene /MeOH	Br	75	120	1+0.32	0	45	53	0	1	1	
6	25	Toluene /MeOH	Br	75	130	1+0.32	0	43	53	0	1	2	
7	20	Toluene /MeOH	Br	75	100	2+0.64	0	63	34	1	1	2	
8	63	Toluene /MeOH	Br	75	110	2+0.64	0	50	47	1	1	1	
9	105	Toluene /MeOH	Br	75	120	2+0.64	0	26	70	2	2	1	
10	2	Toluene /MeOH	Cl	75	100	1+0.32	0	98	1	0	0	0	
11	3	Toluene /MeOH	Cl	75	120	1+0.32	0	99	1	0	0	0	
12	4	Toluene /MeOH	Cl	75	140	1+0.32	0	93	6	0	0	0	
13	3	Toluene /MeOH	Cl	75	100	2+0.64	0	99	1	0	0	0	
14	4	Toluene /MeOH	Cl	75	120	2+0.64	0	93	7	0	0	0	
15	6	Toluene /MeOH	Cl	75	140	2+0.64	0	91	8	0	0	0	
16	3	ACN	Br	75	100	1+0.32	0	68	19	5	0	7	
17	27	ACN	Br	75	120	1+0.32	3	37	26	28	3	3	
18	29	ACN	Br	75	140	1+0.32	0	15	74	9	2	1	
19	22	ACN	Br	75	100	2+0.64	0	37	50	8	2	3	

Table 2.4 continued

#	YIELD (%)	SOLVENT	X	T _{CHIP1} (°C)	T _{CHIP2} (°C)	T _R (MIN, CHIP1+2)	% [1]	% [3A/B]	% [4]	% [5]	% [7]	% [6]
20	33	ACN	Br	75	120	2+0.64	0	20	70	7	2	1
21	37	ACN	Br	75	140	2+0.64	0	10	78	9	2	1
22	3	ACN	Cl	75	100	1+0.32	1	97	1	0	0	1
23	3	ACN	Cl	75	120	1+0.32	0	98	2	0	0	0
24	5	ACN	Cl	75	140	1+0.32	0	94	6	0	0	0
25	3	ACN	Cl	75	100	2+0.64	0	98	2	0	0	0
26	4	ACN	Cl	75	120	2+0.64	0	95	5	0	0	0
27	6	ACN	Cl	75	140	2+0.64	0	89	10	0	0	0
28	2	Toluene /NMP	Cl	75	100	1+0.32	0	62	32	0	2	4
29	4	Toluene /NMP	Cl	75	120	1+0.32	1	55	38	0	2	4
30	10	Toluene /NMP	Cl	75	140	1+0.32	0	62	37	0	1	0
31	5	Toluene /NMP	Cl	75	100	2+0.64	0	60	38	0	1	1
32	8	Toluene /NMP	Cl	75	120	2+0.64	0	52	47	0	1	0
33	14	Toluene /NMP	Cl	75	140	2+0.64	0	27	71	0	2	0
34	19	Toluene /NMP	Br	75	100	1+0.32	0	0	93	1	2	4
35	29	Toluene /NMP	Br	75	120	1+0.32	0	0	93	1	4	2
36	16	Toluene /NMP	Br	75	140	1+0.32	0	0	92	1	4	3
37	7	Toluene /NMP	Br	75	100	2+0.64	0	0	89	3	4	4
38	4	Toluene /NMP	Br	75	120	2+0.64	2	4	49	24	4	17

2.6 References

- [1] Adamo, A.; Beingessner, R. L.; Behnam, M.; Chen, J.; Jamison, T. F.; Jensen, K. F.; Monbaliu, J. M.; Myerson, A. S.; Revalor, E. M.; Snead, D. R.; Stelzer, T.; Weeranoppanant, N.; Wong, S. Y.; Zhang, P. *Science* **2016**, 352 (6281), 61-67
- [2] Bédard, A.; Longstreet, A. R.; Britton, J.; Wang, Y.; Moriguchi, H.; Hicklin, R. W.; Green, W. H.; Jamison, T. F. *Bioor. Med. Chem.* <http://dx.doi.org/10.1016/j.bmc.2017.02.002>
- [3] Baumann, M.; Baxendale, I. R. *Beilstein J. Org. Chem.* **2015**, 11, 1194-1219
- [4] Malet-Sanz, L.; Susanne, F. *J. Med. Chem.* **2012**, 55, 4062-4098
- [5] McQuade, D. T.; Seeberger, P.H. *J. Org. Chem.* **2013**, 78, 6384-6389
- [6] Chen, P. *Angew. Chem. Int. Ed.* **2003**, 42, 2832–2847
- [7] Santos, L. S.; Rosso, G. B.; Pilli, R.A.; Eberlin, M. N. *J. Org. Chem.* **2007**, 72, 5809–5812
- [8] Huang, G.; Li, G.; Dukan, J.; Ouyang, Z.; Cooks, R. G. *Angew. Chem. Int. Ed.* **2011**, 50, 2503–2506
- [9] Banerjee, S.; Zare, R. N. *Angew. Chem. Int. Ed.* **2015**, 54, 14795-14799
- [10] X. Yan, R. M. Bain, R. G. Cooks, *Angew. Chem. Int. Ed.* **2016**, 55, 12960
- [11] Bain, R. M.; Pulliam, C. J.; Cooks, R. G. *Chem. Sci.* **2015**, 6, 397-401
- [12] Bain, R. M.; Pulliam, C. J.; Thery, F.; Cooks, R. G. *Angew. Chem. Int. Ed.* **2016**, 55, 10478-10482
- [13] Wleklinski, M.; Falcone, C. E.; Loren, B. P.; Jaman, Z.; Iyer, K.; Ewan, H. S.; Hyun, S. H.; Thompson, D. T.; Cooks, R. G. *Eur. J. Org. Chem.* **2016**, 33, 5480-5484
- [14] Roughley, S. D.; Jordan, A. M. *J. Med. Chem.* **2001**, 44, 3451-3479
- [15] Maslanka, A.; Krzek, J.; Szlosarczyk, M.; Zmudzki, P.; Wach, K. *Int. J. Pharm.* **2013**, 455, 104-112

CHAPTER 3. HIGH THROUGHPUT EXPERIMENTATION USING DESI-MS TO GUIDE CONTINUOUS-FLOW SYNTHESIS FOR N-ALKYLATION REACTIONS

This chapter was originally published in *Scientific Reports*: Loren, B. P.; Ewan, H. S.; Avramova, L.; Ferreira C. R.; Sobreira, T. J. P.; Yammine, K.; Liao, H.; Cooks, R. G.; Thompson, D. H. *Sci. Rep.*, **2019**, 9, 14745.

3.1 Introduction

Application of continuous-flow technologies has attracted the attention of chemists and the chemical and pharmaceutical industries in recent years due to desirable qualities compared to batch technologies such as improved safety, lower environmental factor (E-factor), amenability to automation, compactness, and facile reactor reconfiguration.¹⁻⁴ Additionally, the superior mixing, improved heat and mass transfer, ease of scaling, and control over other process parameters in continuous-flow can lead to more efficient reactions and potentially even enable chemistries not possible in batch.^{1-2,5} Additional advantages of continuous-flow technologies are their capacity for integration of reaction, purification, and analytics into a single compact automated system.⁶⁻⁹ Although continuous-flow methods can enable the execution of efficient reactions in short residence times, the optimization process can still be costly and time consuming if many reagent types and conditions must be screened. Some laboratories have addressed this issue by integrating continuous-flow methods with on-line reaction monitoring to develop self-optimizing synthesis systems.¹⁰⁻¹² High throughput experimentation (HTE) also has tremendous potential to impact reaction selection, optimization, and discovery efforts.¹³⁻¹⁵

High throughput experimentation is transforming the drug discovery process.¹⁶⁻¹⁹ In much the same way that these tools have accelerated drug development, HTE in organic reaction exploration is poised to drastically boost the efficiency of reaction discovery, route selection, and

step optimization. Several different approaches have been used to screen reactions in both batch¹³-¹⁴ and continuous-flow^{11,15,20} under high throughput conditions. One attractive approach involves accelerated reaction screening in microdroplets to inform scaled up synthesis.^{6,21-26} Our efforts are particularly focused on utilizing reaction acceleration to inform continuous-flow syntheses.^{6,21-23} We have recently reported an extension of this approach to a high throughput format using desorption electrospray ionization mass spectrometry (DESI-MS).²⁷ This system is capable of running several thousand reactions per hour in an automated fashion. We now report the application of this HTE method to guide the optimization of microfluidic reactions. Batch reactions in well plate arrays were used to examine the connection between reactions run with the DESI, batch, and continuous-flow reactors. Each combination of substrate, stoichiometry, and solvent was first screened with the high throughput accelerated DESI reactor. Reaction mixtures for DESI experiments were prepared with a Beckman Coulter Biomek FX liquid handling robot and subsequently transferred to a porous PTFE substrate using a magnetic pin tool to print 50 nL of each reaction mixture onto the substrate surface. This plate, with each reaction spot containing less than 1 µg of material, was then transferred to the mass spectrometer for DESI-MS imaging of the surface. As the plate is rastered underneath the solvent sprayer, the material on the surface is desorbed and secondary droplets are collected and rapidly analyzed by the mass spectrometer in a manner that has the potential to accelerate the reaction of interest.²⁷ The speed and compatibility of the HTE platform with automated DESI-MS analysis contrasts sharply with the traditional process of identifying preferred reaction conditions through an iterative series of batch experiments.

The main strategy of this HTE approach is to utilize the highest throughput tool in the HTE system, DESI-MS, to produce an initial reactivity heat map, by-product profiles, and structural

analyses of the reaction outcomes via MS/MS.²⁷ The remarkable throughput of this system is enabled by the robotic preparation of reaction arrays at high densities and by the possible acceleration of the reactions themselves in thin films or in charged microdroplets.^{25,27} Whether each reaction is accelerated in a thin film or a microdroplet or is simply occurring during the initial mixing remains ambiguous, but the utility of the technique overall is not necessarily dependent on this distinction and is thus not the focus of this work. Once the heat map has been produced, reaction conditions corresponding to the “yes” areas of the map may then be elevated to the next level of HTE, while the “no” conditions are abandoned. A more limited range of “yes” conditions can then be tested in small volume batch reactions prepared in microtiter plates as an intermediate step to help validate the DESI-MS experiment and potentially provide more textured data with respect to temperature effects and product quantitation. Data from this series of experiments can then be used to guide reaction optimization to achieve the highest yielding transformations under continuous-flow conditions in an efficient manner. The “no” conditions that are abandoned in this way represent a significant reduction in manpower and material waste, as the need to review those conditions in continuous flow or batch experiments is eliminated.

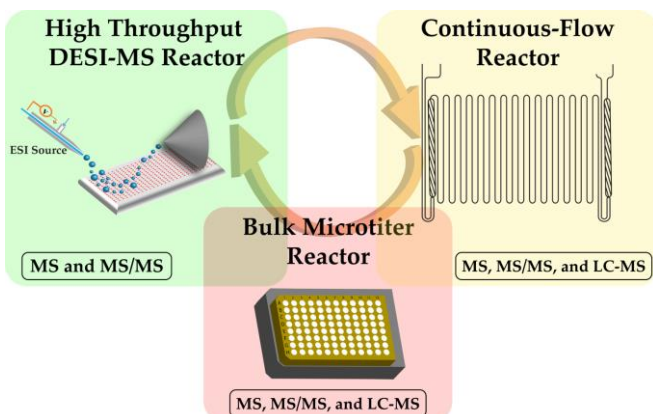


Figure 3.1. Conceptual representation of the reactor types and exchange of reactivity data between the (i) accelerated droplet reactor (ii) bulk microtiter reactor and (iii) continuous-flow reactor. Analytical tools used to monitor the reaction outcomes in each case are also shown.

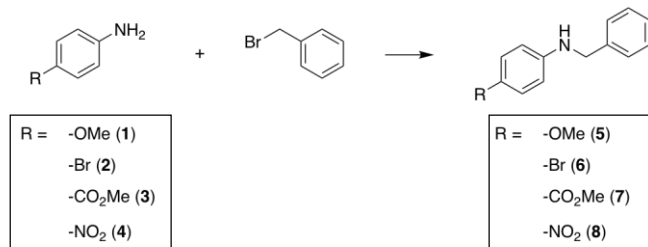
In order to build the necessary confidence in this heat map-based reaction pruning approach, it is important to demonstrate that reactivity trends are consistent across each platform. Since the goal of this HTE approach is to guide downstream optimization and scaling by narrowing down the potential reaction space, it is not essential to quantitatively predict reaction outcomes in the DESI-MS “yes/no” evaluation. The focus instead is on rapidly identifying the presence or absence of target compound and/or reaction byproducts.

N-alkylation reactions were chosen as the test case for this system due to their high relevance in medicinal chemistry.²⁸ Trends in reactivity were explored in each reactor type with varying substrate, solvent, stoichiometry and temperature (the latter only in the cases of bulk microtiter and continuous-flow). Our first experiment evaluated aniline reactivity as a function of varying electron demand substituents using a common electrophile, benzyl bromide. Once an initial correlation between the screening approaches was established, we expanded the scope of amine types using both the high throughput DESI and continuous-flow experiments. Scale up of a reaction in continuous-flow based on the outcome of this larger experiment was also demonstrated.

3.2 Results and Discussion

3.2.1 Aniline Reactivity Screen

We began our search of reactivity trends using four anilines having para-substituents that imposed varying electronic demand on the amine nucleophile (Scheme 3.1). It is well known that aniline nucleophilicity is strongly influenced by substituents that alter the electron density in the aromatic ring. We chose this transformation as a test case to establish whether the expected reactivity trends would be consistent across each reactor platform. Each aniline was mixed with benzyl bromide in three solvents (ACN, Toluene, DMSO) at three stoichiometries (10:1, 1:1, 1:10). Observation of the expected trends across the different reactor platforms would serve as the first indication that DESI and/or batch pre-screening may offer valid predictions for the corresponding continuous-flow reaction outcomes.



Scheme 3.1. N-alkylation reactions executed on the DESI, batch microtiter, and continuous-flow reactor platforms.

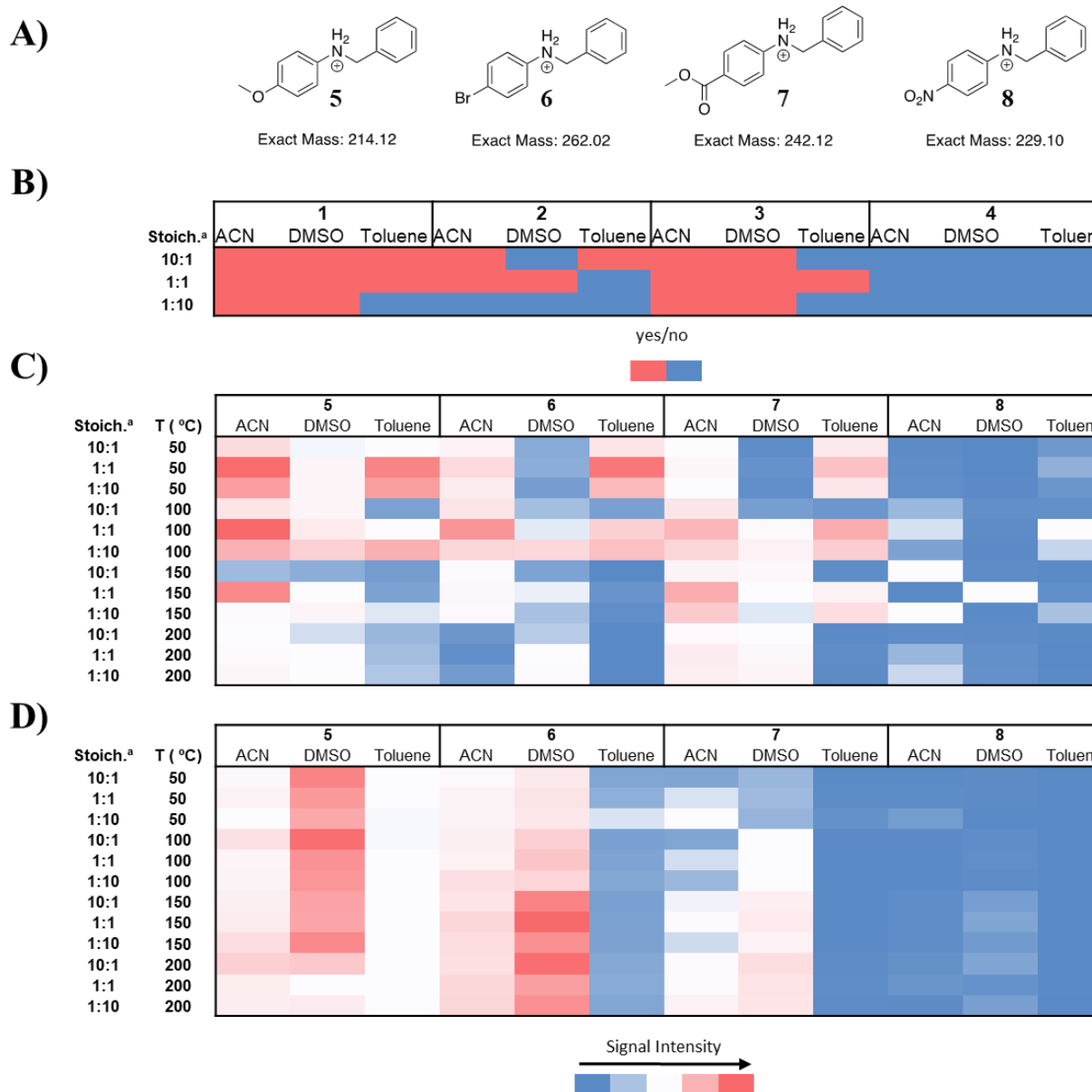


Figure 3.2. (A) Structures of the reaction products. Heat map representations of (B) yes/no reaction outcomes based on ion intensities in the high throughput DESI-MS experiment, (C) LC/MS quantitation of the batch experiment, and (D) LC/MS quantitation of the continuous-flow experiment. ^aStoichiometries are reported as ratios of aniline:benzyl bromide.

The high throughput DESI experiment was carried out by preparing reaction mixtures in standard polypropylene 384-well plates using a Beckman Coulter Biomek FX liquid handling robot. A magnetic pin tool with 50 nL slotted pins was then interfaced with the constant volume transfer arm of the robot to deposit a small volume of each reaction mixture onto a porous PTFE

substrate. This plate, with each spot representing a unique set of reaction conditions, was then transferred to the DESI-MS for analysis immediately following its preparation. In a separate experiment, the same set of conditions, rather than being spotted onto the porous PTFE plate, were deposited into glass vials inserted within 96-well aluminum blocks for high throughput batch microtiter reaction screening. These reaction blocks were compression sealed with a PFA-lined silicone mat, allowing the reactions to be heated at reflux. Four such plates were prepared from a master plate and heated at 50, 100, 150, and 200 °C, respectively, for 30 minutes, followed by dilution into ACN to quench the reactions prior to storage at -80 °C for subsequent analysis by ESI-MS. The continuous-flow experiments were executed in 10 µL glass reactor chips mounted on a Chemtrix Labtrix S1 reactor system. The flow reactions were similarly quenched by dilution into ACN and storing at -80 °C until ESI-MS analysis. Since the goal of this initial experiment was to track reactivity trends rather than optimize individual transformations, the continuous-flow experiments were carried out with a constant short residence time of 30 sec. Quantitation of the batch and continuous-flow reactions was conducted using LC-MS and referenced to an external calibration curve to mitigate concerns that the observed conversion trends might be dependent on the varying ionization efficiencies of the anilines.

Heat map representations of all three experiments, based on product ion intensities for the DESI experiment and LC/MS determined concentrations for the batch microtiter and continuous-flow experiments, are shown in Figure 3.2. The color scale for each of these heat maps is set to the same range of signal intensities across the entire heat map. For the DESI heat map, a binary “yes/no” scale was used with a threshold of 30 ion counts for the target mass to charge ratio (m/z), while the other heat maps are shown as a concentration-based color gradients. The high throughput DESI-MS experiment (Figure 3.2B) was conducted at a 1,536 well plate density using 50 nL

transfer pins to deposit the sample onto a porous PTFE plate that was cut to the dimensions of a standard microscope slide. This experiment showed that p-anisidine (1) was readily monoalkylated, whereas p-bromobenzene (2) and methyl 4-aminobenzoate (3) had some conversion to product, and p-nitroaniline (4) produced minimal monoalkylation product. Further, there appears to be a strong solvent effect in the case of **3**, with ACN and DMSO favoring product formation, whereas toluene failed to produce a significant amount of product. These same substrate and solvent trends were observed in the continuous-flow experiments (Figure 3.2D). It is notable that these trends appear to be consistent whether the continuous-flow data was analyzed qualitatively (ESI-MS) or quantitatively (LC-MS), suggesting that the observed conversion trend was not merely an artifact of ionization efficiency. This important finding suggests that DESI-MS may be a useful HTE tool for reaction optimization.

While the substrate and solvent trends appear to translate well for reactions run under DESI and flow conditions, there is some disagreement between the batch and flow results. This is particularly true when considering the reactivity trends as a function of temperature. The continuous-flow reactions showed a strong temperature dependence, wherein higher temperatures provided higher yields, while lower temperatures were more favorable under batch conditions. We attribute these findings to the longer reaction times used in the batch experiment (30 min), resulting in thermal degradation of the products and/or starting materials when heated to 150 or 200 °C. To further probe this, a series of continuous-flow experiments were executed at 200 °C using an 8 minute residence time. Comparison of the full mass spectra for these flow experiments and batch experiments showed significantly reduced product formation relative to the shorter timeframe flow reactions. We infer from these findings that thermal degradation was the likely source of ineffective data translation between the batch microtiter and continuous-flow experiments. These

observations also highlight an inherent limitation in batch HTE. Even though the aluminum blocks enable heating of the reaction arrays at reflux, heat transfer is much slower and less well controlled in these reactors compared to continuous-flow reactors. This, in turn, leads to less control over reaction conditions, resulting in the thermal degradation that was observed in the mass spectra.

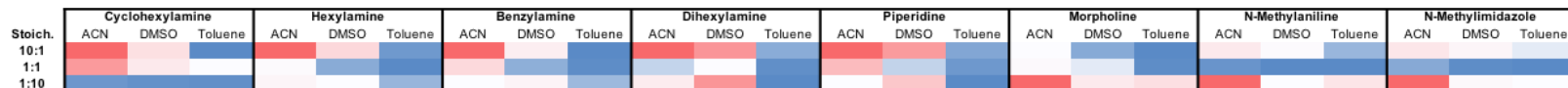
In spite of this complication, the reactivity trend fidelity observed using the DESI and continuous-flow reactors suggests that DESI-MS HTE represents a path for dramatically increasing the rate of reaction optimization. Although the DESI reactor is not able to heat reactions, the ultimate goal of the DESI experiment is to deploy its thousands-of-reactions per hour throughput to rapidly scout out a vast chemical reactivity space to identify a significantly smaller number of reactions that can then be carried forward for optimization and scaling.

3.2.2 Expanded N-alkylation Screen

The aniline experiment established a correlation between the reaction outcomes in high throughput DESI and continuous-flow reactors, thereby confirming the utility of DESI as a predictive tool for judging the likely outcome of flow experiments. These encouraging results lead us to expand the scope of amine substrates to determine whether the correlations would hold for a more diverse family of amines. Their reactivity was surveyed using DESI and continuous-flow to determine whether the observed reactivity trends would translate well across these platforms. Given the degradation complications observed with the previous batch microtiter experiments, this reactor was not utilized in these expanded N-alkylation experiments. Each combination of substrate, stoichiometry, and solvent was again screened under the same DESI conditions as in the previous experiments, except that a PTFE plate the size of a standard well plate was used. The reactions in this case were spotted in quadruplicate using 50 nL slotted pins to produce a plate at standard 1,536 well density. Rhodamine was incorporated on the plate as a fiducial marker to allow

in-house developed software to determine the exact x and y coordinates for each reaction spot. Heat maps were again generated for both the DESI-MS and continuous-flow datasets (Figure 3.3). The heat maps for this dataset are based on ion intensities and organized by the different amine starting materials. Conditional color formatting was reset for each amine to avoid a misinterpretation of the heat maps due to trends based on differences in ionization efficiency rather than chemical reactivity. These DESI heat maps are displayed as a multi-color scale in the same manner as the flow reaction heat map. This is because with the color gradient set for each amine individually, the threshold for a yes/no is different for each amine. Since we are not comparing different substrates to each other in this experiment, we are able to more easily observe any solvent and stoichiometry trends for each individual amine in this way. Given that the main objective of this experiment was to streamline the optimization of any one of these reactions, reporting the data in this manner most clearly illustrates the high throughput potential of the method.

A)



B)

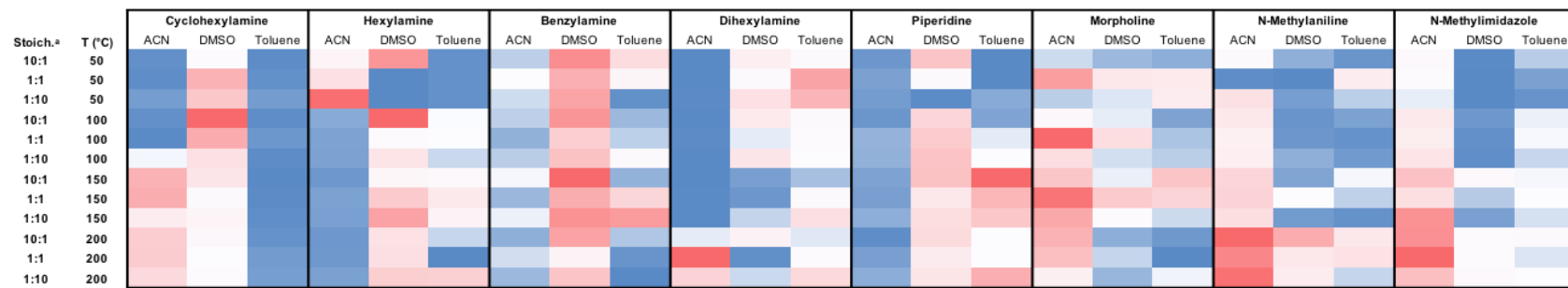


Figure 3.3. Heat map representations of (A) ion intensities in the high throughput DESI experiment and (B) ion intensities in the continuous-flow experiment. *Stoichiometries are reported as ratios of amine:benzyl bromide. *Bold outlines indicate regions of the heat map where the conditional color formatting was set.

The DESI results again suggest that ACN is the best solvent in most cases, while DMSO will generally be superior to toluene for these reactions. Although this solvent trend did not precisely track across all of the continuous-flow reactions, it translated well overall. Specifically, ACN was the hottest spot in the continuous-flow experiments for 5 out of 8 amines and DMSO was the hottest spot for 2 out of 8 amines. Piperidine was the only case where toluene was the hottest spot in the continuous-flow dataset. Although piperidine is an example of a case where the DESI and continuous-flow experiments are misaligned, the DESI-MS results indicated a lower overall ion intensity in all of its reactions compared to the other amines. Therefore, while the reactivity trends across the solvents did not appear to fully translate in this case, the DESI-MS results did reveal that the overall reactivity of piperidine was lower than the other amines. The likelihood that this is the source of the inconsistency is supported by the finding that significant product formation in this reaction only occurred at elevated temperature in continuous-flow.

3.2.3 Using HTE to Scale a Reaction

Since our ultimate goal was the selection from a large set of reaction outcomes a smaller and more manageable optimal set of conditions, we chose a single substrate, cyclohexylamine, to test the entire HTE workflow from DESI-MS to scalable product formation in continuous-flow. The DESI experiment showed ACN as the optimal solvent, with DMSO as second best. Based on the DESI and microfluidic experiments, a focused set of microfluidic reactions were performed in ACN and DMSO with varying residence times at an increased concentration of 1 M to better reflect continuous production conditions. The ACN reaction in continuous-flow, however, was a practical failure due to precipitation and clogging of the reactor chip by the monoalkylated product at this increased concentration, thus leaving DMSO as the only viable option for optimizing production in continuous-flow. In this case, we were able to reduce the search by one third of possible

conditions in our predefined chemical space. In the large data sets that this system is designed for, such a reduction in search space may represent a significant time savings and reduction in chemical waste generated. The yield of these reactions was determined by LC-MS quantitation, with the highest yields occurring at a residence time of 30 seconds and a temperature of 100 °C, translating to 56.6% yield and a production rate of 42.8 mg/hr.

Table 3.1. Optimization of the reaction between cyclohexylamine and benzyl bromide.
Stoichiometries are reported as ratios of amine:benzyl bromide.

Entry	R _T (sec)	Stoich. ^a	Temp. (°C)	Yield (%)
1	15	1:2	100	29.8
2	15	1:1	100	34.3
3	15	2:1	100	50.8
4	30	1:2	100	56.6
5	30	1:1	100	47.1
6	30	2:1	100	28.6
7	60	1:2	100	24.3
8	60	1:1	100	29.2
9	60	2:1	100	43.2

3.2.4 Conclusions

The utility of DESI-MS as a HTE tool for rapidly evaluating large numbers of reactions to help guide condition selection and optimization for continuous-flow synthesis was demonstrated. Although this HTE system is not capable of quantitatively determining the optimal condition for scale-up, it is able to narrow down the number of conditions that need to be evaluated during scaling efforts. A series of experiments were performed to test how well reactivity trends observed using the DESI and batch microtiter reactors can be used to identify the best synthesis conditions for use in a continuous-flow reactor. N-alkylation reactions were used as the test bed for these experiments, first using a focused screen of anilines having varied electron demand on the aromatic

ring. This experiment provided encouraging evidence that reactivity trends observed as a function of solvent in the accelerated DESI reactor were able to translate well to continuous-flow reaction conditions. Translation of data from the batch microtiter in this case was less effective, but this appears to be due to degradation of material at the highest temperatures screened. While this represented a limitation of our batch microtiter reactor platform under the conditions employed, it is still a valuable tool for examining reactions run under bulk conditions that are commonly found in the literature.

DESI and continuous-flow reactions on a broader scope of amines were then performed. These experiments established that the reactivity trends observed with the aniline experiments also translated well to a broader scope of amines. While the reactivity heat map of each individual reaction did not completely track across the two platforms, the general trend of more polar solvents being preferred did translate. This is an important point since the goal of the DESI reaction platform is not to provide a single reaction condition that will be executed at scale, but rather to take an extremely large chemical reaction space and narrow it to something that can be more manageably evaluated in continuous-flow to discover the optimal conditions needed for scaling. To demonstrate this concept, a single amine, cyclohexylamine, was chosen for optimization and scale up in continuous-flow. The flow reaction optimization process resulted in a method capable of producing a 56.6 % yield of the benzylated product at a residence time of 30 sec and an amine:benzyl bromide ratio of 1:2, representing a production rate of 42.8 mg/hr in a 10 μ L reactor chip. In implementing our DESI-MS guided reaction selection model, we reduced the search space for the optimized reaction by one third. As our system develops and data sets grow, such a reduction in search space may represent a significant savings in time, energy, and chemical waste.

This study demonstrates the potential of high throughput reaction screening with DESI-MS to accelerate route selection and optimization. While we found DESI-MS to narrow the scope of possibilities for reaction selection with some parameters such as solvent, others like stoichiometry and temperature still required screening in a microfluidic reactor to optimize. While it has been demonstrated as useful in the translation of high throughput data to continuous-flow data in the case of N-alkylation reactions, in order to more fully establish its usefulness as a screening tool for organic reactions, the scope of chemistry conducted with this platform must be further expanded. Efforts devoted to the expansion of HTE throughput and refinement of the hardware and software for the automation of both reaction preparation and analysis are important next steps that are ongoing.

3.3 Materials and Methods

3.3.1 General Procedure for DESI-MS Experiments

The DESI-MS experiments were conducted as described previously.²⁷ A Biomek FX liquid handling robot (Beckman Coulter) was used to distribute reaction mixtures into master well plates (either 96 or 384 well plates, depending on the scope of the experiment). The 96-tip transfer pod (pod1) and the Span-8 transfer pod (pod2) were both utilized to generate the target set of reaction conditions. The final reaction concentration for all DESI-MS experiments was 50 mM (20-30 μ L in the final 384 well master plate). A magnetic pin tool (V&P Scientific, Inc.) was interfaced with pod1 of the liquid handling robot and used to transfer 50 nL volumes of reaction mixtures from the master well plate to the porous PTFE surface for DESI-MS. A commercial DESI source (Prosolia, Inc.) and a Thermo LTQ linear ion trap were utilized to execute the DESI-MS experiment. Experiments were conducted in positive-ion mode (m/z 50-500) with pure methanol

as the spray solvent (3 μ L/min). Parameters for the mass spectrometer and speed of the DESI stage were optimized previously.²⁷ In-house software was used to process the data and generate spreadsheets from which heat maps were prepared.

3.3.2 General Procedure for Qualitative MS Analysis

Mass spectral analysis was performed for each flow and batch reaction sample using a Thermo TSQ triple quadrupole mass spectrometer (Thermo Fisher Scientific) equipped with an autosampler and electrospray (ESI) ionization. Reaction samples were diluted 1:1000 into ACN upon collection and cooled to -80°C to quench the reactions before warming to room temperature immediately prior to analysis. The distance between the tip of the spray emitter and the ion transfer capillary to the MS was kept constant at ca. 1.5 cm. Experiments were performed using a Thermo-Fisher HESI-II probe and Ion Max ion source. A spray voltage of 3.5 kV was used for all analyses. Positive-ion mode was used for all analyses.

3.3.3 Quantitative LC/MS Analysis

Quantitative measurements were carried out with an Agilent 6460 triple quadrupole LC/MS with an Agilent Series 1200 degasser, binary pump, and autosampler. An XBridge Phenyl 3.5 μ m 2.1x100 mm column was used to separate the aniline products, while an Atlantis dC18 3 μ m 2.1x150 mm column was used to separate the cyclohexylamine products. The elution used a gradient of ACN:H₂O with 0.1 % formic acid. Calibration curves were made using standards of the respective products.

3.3.4 General Procedure for Bulk Microtiter Experiments

A Biomek FX liquid handling robot was used to distribute reaction mixtures into aluminium well plates fitted with glass vials (Analytical Sales & Services, Inc.). A master plate was prepared with varying substrates, solvents, and stoichiometries and then distributed into four identical plates that were sealed with a PFA film and two silicone rubber mats before heating for 30 min at 50, 100, 150, and 200 °C, respectively. Each reaction vial was prepared at 50 mM and contained 50 µL of reaction mixture. After allowing the plates to cool, the Biomek FX was used to dilute the reaction mixtures to 500 µM in ACN. A Thermo TSQ mass spectrometer equipped with an autosampler was used for the qualitative analysis of these reactions. The protocol for quantitative analysis is described below.

3.3.5 General Protocol for Continuous-Flow Experiments

All microfluidic reactions were carried out using a Chemtrix Labtrix S1 system equipped with 3223 glass reactor chips. Solutions of 0.05 M amines and 0.05 M benzyl bromide in Toluene, ACN and DMSO were prepared. Syringes were loaded with each of these solutions and positioned on the first two inlets of a 10 µL Chemtrix 3223 chip. The reactants were engaged with 30 s residence times at temperatures of 50, 100, 150, and 200 °C. Samples were collected and immediately diluted 1:1000 in ACN and stored at -80 °C prior to analysis.

3.3.6 Continuous-Flow Degradation Experiments

Reactions were carried out using a Chemtrix Labtrix S1 system equipped with 3223 glass reactor chips as described above, except that the reactants were flowed with 8 minutes residence times at 200 °C. Samples were then handled as described above.

3.3.7 Continuous-Flow Optimization Experiments

Reactions were carried out using a Chemtrix Labtrix S1 system equipped with 3223 glass reactor chips as described above, except that solutions of 1 M amine and 1 M benzyl bromide in Toluene, ACN and DMSO were used. The reactants were flowed with 15, 30, and 60 s residence times at temperatures of 100°C before collecting and handling as described above.

3.4 References

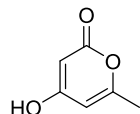
- [18] Gutmann, B.; Cantillo, D.; Kappe, C. O. *Angew. Chem. Int. Ed.* **2015**, 54, 6688-728
- [19] Jensen, K. F.; Reizman, B.; Newman, S. G. *Lab Chip.* **2014**, 14, 3206-3212
- [20] Ouchi, T.; Mutton, R. J.; Rojas, V.; Fitzpatrick, D. E.; Cork, D. G.; Battilocchio, C.; Ley, S. V. *ACS Sustain. Chem. Eng.* **2016**, 4, 1912-1916
- [21] Fitzpatrick, D. E.; Battilocchio, C.; Ley, S. V. *ACS Cent. Sci.* **2016**, 2, 131-138
- [22] Kim, H.; Min, K. I.; Inoue, K.; Im do, J.; Kim, D. P.; Yoshida, J. *Science* **2016**, 352, 691-694
- [23] Loren, B. P.; Wleklinski, M.; Koswara, A.; Yammine, K.; Hu, Y.; Nagy, Z. K.; Thompson, D. H.; Cooks, R. G. *Chem. Sci.* **2017**, 8, 4363-4370
- [24] Mascia, S.; Heider, P. L.; Zhang, H.; Lakerveld, R.; Benyahia, B.; Barton, P. I.; Braatz, R. D.; Cooney, C. L.; Evans, J. M. B.; Jamison, T. F.; Jensen, K. F.; Myerson, A. S.; Trout, B. L. *Angew. Chem. Int. Ed.* **2013**, 52, 12359-63
- [25] Adamo, A.; Beingessner, R. L.; Behnam, M.; Chen, J.; Jamison, T. F.; Jensen, K. F.; Monbaliu, J. C.; Myerson, A. S.; Revalor, E. M.; Snead, D. R.; Stelzer, T.; Weeranoppanat, N.; Wong, S. Y.; Zhang, P. *Science* **2016**, 352, 61-7
- [26] Zhang, P.; Weeranoppanat, N.; Thomas, D. A.; Tahara, K.; Stelzer, T.; Russel, M. G.; O'Mahony, M.; Myerson, A. S.; Lin, H.; Kelly, L. P.; Jensen, K. F.; Jamison, T. F.; Dai, C.; Cui, Y.; Briggs, N.; Beingessner, R. L.; Adamo, A. *Chem. Eur. J.* **2018**, 24, 2776-2784
- [27] Fitzpatrick, D. E.; Battilocchio, C.; Ley, S. V. *Org. Process Res. Dev.* **2016**, 20, 386-394

- [28] Reizman, B. J.; Wang, Y; Buchwald, S. L.; Jensen, K. F. *React. Chem. Eng.* **2016**, 1, 658-666
- [29] Parrott, A. J.; Bourne, R. A.; Akien, G. R.; Irvine, D. J.; Poliakoff, M. *Angew. Chem. Int. Ed.* **2011**, 50, 3788-3792
- [30] Troshin, K.; Hartwig, J. F. *Science* **2017**, 357, 175-181
- [31] Buitrago Santanilla, A.; Regalado, E. L.; Pereira, T.; Shelvin, M.; Bateman, K.; Campeau, L. C.; Scneeweis, J.; Berrit, S.; Shi, Z. C.; Nantermet, P.; Liu, Y.; Helmy, R.; Welch, C. J.; Vachal, P.; Davies, I. W.; Cernak, T.; Dreher, S. D. *Science* **2015**, 347, 49-53
- [32] Perera, D.; Tucker, W. J.; Brahmbhatt, S.; Helal, C. J.; Chong, A.; Farrell, W.; Richardson, P.; Sach, N. W. *Science* **2018**, 359, 429-434
- [33] Mayr, L. M.; Bojanic, D., *Curr. Opin. Pharmacol.* **2009**, 9, 580-588 (2009).
- [34] Koehn, F. E., High impact technologies for natural products screening. In Natural Compounds as Drugs Volume I, Petersen, F.; Amstutz, R., Eds. Birkhäuser Basel: Basel, 2008; pp 175-210.
- [35] Janzen, W. P. *Chem. Biol.* **2014**, 21, 1162-1170
- [36] Syahir, A.; Usui, K.; Tomizaki, K.; Kajikawa, K.; Mihara, H.; *Microarrays* **2015**, 4, 228-244
- [37] Reizman, B. J.; Jensen, K. F., *Acc. Chem. Res.* **2016**, 49, 1786-1796
- [38] Wleklinski, M.; Falcone, C. E.; Loren, B. P.; Jaman, Z.; Iyer, K.; Ewan, H. S.; Hyun, S.; Thompson, D. H.; Cooks, R. G. *Eur. J. Org. Chem.* **2016**, 2016, 5480-5484
- [39] Ewan, H. S.; Iyer, K.; Hyun, S.; Wleklinski, M.; Cooks, R. G.; Thompson, D. H. *Org. Process Res. Dev.* **2017**, 21, 1566-1570
- [40] Falcone, C. E.; Jaman, Z.; Wleklinski, M.; Koswara, A.; Thompson, D. H.; Cooks, R. G. *Analyst* **2017**, 142, 2836-2845
- [41] Bain, R. M.; Pulliam, C. J.; Cooks, R. G. *Chem. Sci.* **2015**, 6, 397-401
- [42] Yan, X.; Bain, R. M.; Cooks, R. G. *Angew. Chem. Int. Ed.* **2016**, 55, 12960-12972
- [43] Banerjee, S.; Zare, R. N., *Angew. Chem. Int. Ed.* **2015**, 54, 14795-14799
- [44] Wleklinski, M.; Loren, B. P.; Ferreira C. R.; Jaman, Z.; Avramova, L.; Sobreira, T. J. P.; Thompson, D. H.; Cooks, R. G. *Chem. Sci.* **2018**, 9, 1647-1653
- [45] Roughley, S. D.; Jordan, A. M., *J. Med. Chem.* **2011**, 54, 3451-3479

CHAPTER 4. REACTIONS OF BIO-RENEWABLE TRIACTIC ACID LACTONE PRECURSOR EVALUATED USING DESORPTION ELECTROSPRAY IONIZATION MASS SPECTROMETRY HIGH THROUGHPUT EXPERIMENTATION SYSTEM

4.1 Introduction

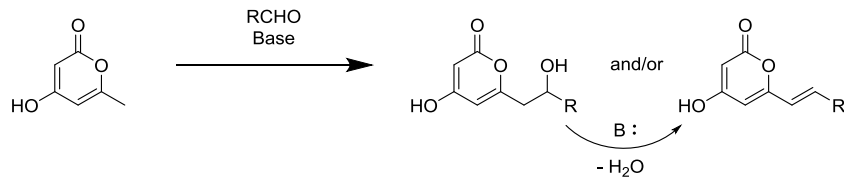
Platform chemicals are versatile molecules that are converted to a wide array of value-added products with applications across various industries. The vast majority of such materials are sourced from petroleum, thus motivating the need to develop renewable and sustainable alternatives. Many bio-renewable molecules have been explored for use as platform chemicals, including various carbohydrate and furan precursors.^{1,2,3} Glycerol is an example of a carbohydrate which has been extensively derivatized into a number of value added products including polymers, coatings, surfactants, and synthetic intermediates.^{4,5} 5-Hydroxymethylfurfural, a dehydration product of fructose, is another example of a biomass derived platform chemical that has been converted into a range of direct replacements for petrochemical products.^{6,7} The polyketide class of natural products possess a highly diverse array of molecular architectures with alternating carbonyl-methylene motifs that make these compounds a promising family of precursors for the development of new platform chemicals.^{3,8}



Scheme 4.1. Triacetic acid lactone (TAL)

Triacetic acid lactone (TAL) is a polyketide that has been produced biosynthetically by Xie and coworkers⁹ via fermentation from glucose using yeast or *E. coli* expressing genetically engineered polyketide synthase. TAL has been converted into a wide array of useful commodity

chemicals, solvents, agrochemicals, and advanced pharmaceutical intermediates using various reaction classes including hydrolysis, hydration, amination, acylation, and aldol condensation.^{8,10-13} Previous reports of aldol reactions with TAL showed that the aldol product may be produced using either two equivalents of base or a single equivalent of base if the TAL alcohol substituent has been protected. Use of more forcing conditions can promote elimination from that aldol product to form a conjugated alkene as shown in Scheme 2.¹³ This study seeks to accelerate the process of developing platform chemicals using aldol reactions of TAL as a model system to expand the scope of products generated by this transformation in a diversity-oriented synthesis effort.



Scheme 4.2. Aldol reaction of TAL and subsequent elimination.

High throughput experimentation (HTE) has been widely and successfully used in the drug discovery and development process.¹⁴⁻¹⁷ We have recently reported the use of desorption electrospray ionization mass spectrometry (DESI-MS) as an HTE tool to accelerate the process of reaction optimization and upscaling.¹⁸⁻²² DESI is an ambient ionization method that uses charged microdroplets of solvent to extract analytes from a surface.^{19,23-25} This approach employs reaction arrays comprised of different reagent combinations, substrate and/or additive stoichiometries, solvent types, incubation times, and reaction temperatures using a Beckman Coulter Biomek i7 liquid handling robot to prepare the reaction mixtures in high density well plates. After preparing the arrays and waiting for the desired incubation time, the reaction arrays are then printed onto a porous polytetrafluoroethylene (PTFE) surface using a magnetic slotted-pin tool array that

withdraws 50 nL per pin when dipped into wells containing the reaction mixture. The pin array is then pressed onto the PTFE surface, depositing a sample of the well mixture containing less than 1 µg of material per spot. This plate is then transferred to the DESI stage of the mass spectrometer, where a stream of charged solvent is sprayed at the surface. The plate is moved beneath this solvent stream, scanning spot-by-spot over the entire reaction printed surface of the PTFE plate. As the stream passes over each reaction spot, the material on the surface is desorbed and secondary droplets enter the MS inlet to be analyzed, producing a full MS spectrum for each point on the surface. These results may then be visualized as a product-ion intensity heat map, revealing successful or unsuccessful conditions to produce the product.^{18, 19} The most successful reactions revealed by this high throughput screen may be validated by performing a scaled up reaction in a microfluidic reactor analyzed by electrospray ionization MS to offer a quick secondary validation of the DESI-MS HTE results as our group has previously demonstrated.²⁶ In addition to validating the HTE results, the ease of automation and simplified optimization and scaling of microfluidic syntheses offers a simplified path forward for further development of derivatives of TAL identified by HTE.^{27,28,29} This technology has the potential to greatly accelerate the development of platform chemicals such as TAL with a minimum input of time and resources, potentially identifying efficient pathways to renewable alternative precursors and end products more rapidly.

4.2 Results & Discussion

4.2.1 First Reaction Set

For the first experiment, aldol reactions of TAL were carried out using each possible combination of three different aldehyde substrates, solvents, stoichiometries, and reaction temperatures for a total of 81 unique reaction conditions. Each reaction was sampled just after

reagent mixing and again after two hours of heating. The reactions were prepared in duplicate wells, with each well printed twice to serve as pinning replicates. With 81 unique reactions sampled at two time points and deposited onto the PTFE plate as four replicates, a total of 648 reaction data points were produced in this experiment. The aldehydes used were benzaldehyde, 4-methoxybenzaldehyde, and hexanal at aldehyde:TAL stoichiometries of 5:1, 1:1, and 1:5. Two equivalents of potassium *t*-butoxide were used relative to TAL. Each reaction was prepared at 50 mM TAL concentration with at least 300 μ L of solution in each well. The i7 liquid handling robot was used to prepare reaction mixtures in 96 well plates with glass inserts that were sealed with PTFE lined silicone rubber mats and heated on home-built constant temperature plates. Each reaction was incubated for 2 hours at room temperature, 50 °C or 100 °C and two 30 μ L samples were withdrawn before and after heating. Each reaction was prepared in duplicate, and upon withdrawing these aliquots from the 96 well plates, they were distributed into 384 well plates to be pinned with the 384 pin tool, thus creating an additional “pinning” replicate. Reaction arrays were then printed onto glass supported PTFE for DESI-MS analysis. The raw MS data was processed with our in-house software and visualized as a heat map as shown in Figure 1.

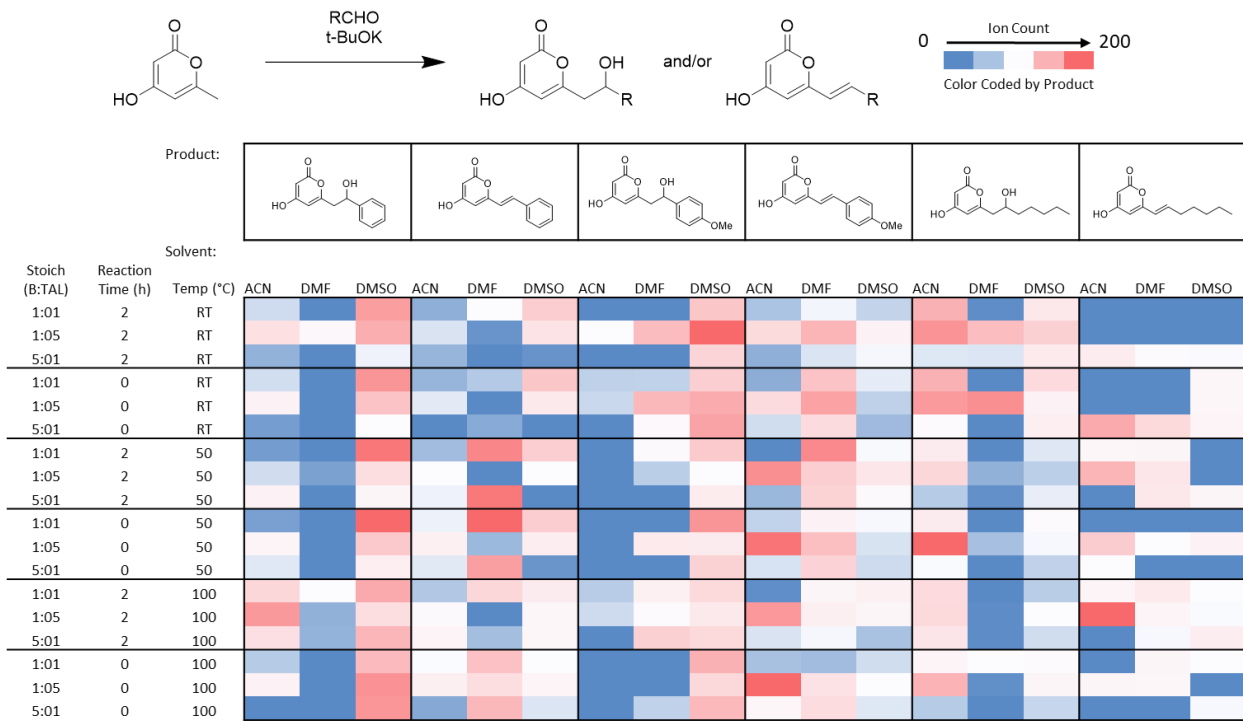
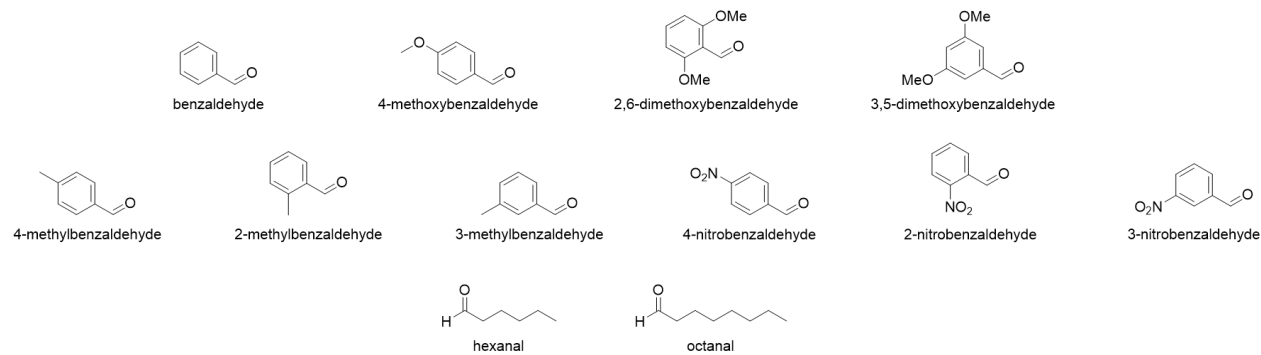


Figure 4.1. Heat map of aldol product signal intensities from aldol reactions of TAL with three substrates, three solvents, three stoichiometries, and three temperatures. Each cell is an average of 4 replicates with normalized MS intensities. Heat maps are color coded by product, separated by dark vertical lines in the table.

The heat map shows hits for both the aldol and elimination products for each of the three aldehyde types. Some reactivity trends also become apparent from examination of the heat maps. In the case of the two aromatic aldehydes, benzaldehyde and 4-methoxybenzaldehyde, DMSO appeared to give better conversion to the alcohol product, whereas DMF appeared to enable greater elimination product formation. These reactions appeared to take place at room temperature as well as at elevated temperatures. For the aliphatic aldehyde hexanal, ACN appeared to be the preferred solvent for generating the aldol product, with the alkene product detected only at higher reaction temperatures. While varying substrate, solvent, and temperature appeared to affect the outcome of the reactions, stoichiometry seemed to have little discernable effect.

4.2.2 Expanded Reaction Set

After this first set of transformations, the substrate scope was expanded to include aldehydes with varying steric and electronic characteristics (Scheme 3). Reaction arrays were prepared and sampled before and after the two-hour heating period as described in the previous experiment. For this experiment, lithium *t*-butoxide (two equivalents) was used as base instead of potassium *t*-butoxide due to the greater solubility of the lithium species in each solvents used in this reaction series. This experiment was also limited to two solvents, two temperatures, and a 1:1 TAL:aldehyde stoichiometric ratio since the previous stoichiometry screen proved uninformative. The solvents selected were DMF, a polar solvent that produced successful reactions in the previous screen, and toluene, a less polar solvent than any that were previously used. During the DESI-MS analysis stage, the negative ionization mode was used, as opposed to positive in the previous experiment, since TAL and its derivatives were more easily detected in negative ion mode. With this simplified array, the experiment explored 48 unique reaction conditions with 8 replicates each, measured at 2 time points for a total of 768 data points.



Scheme 4.3. Aldehyde starting materials used in the TAL reactivity HTE study.

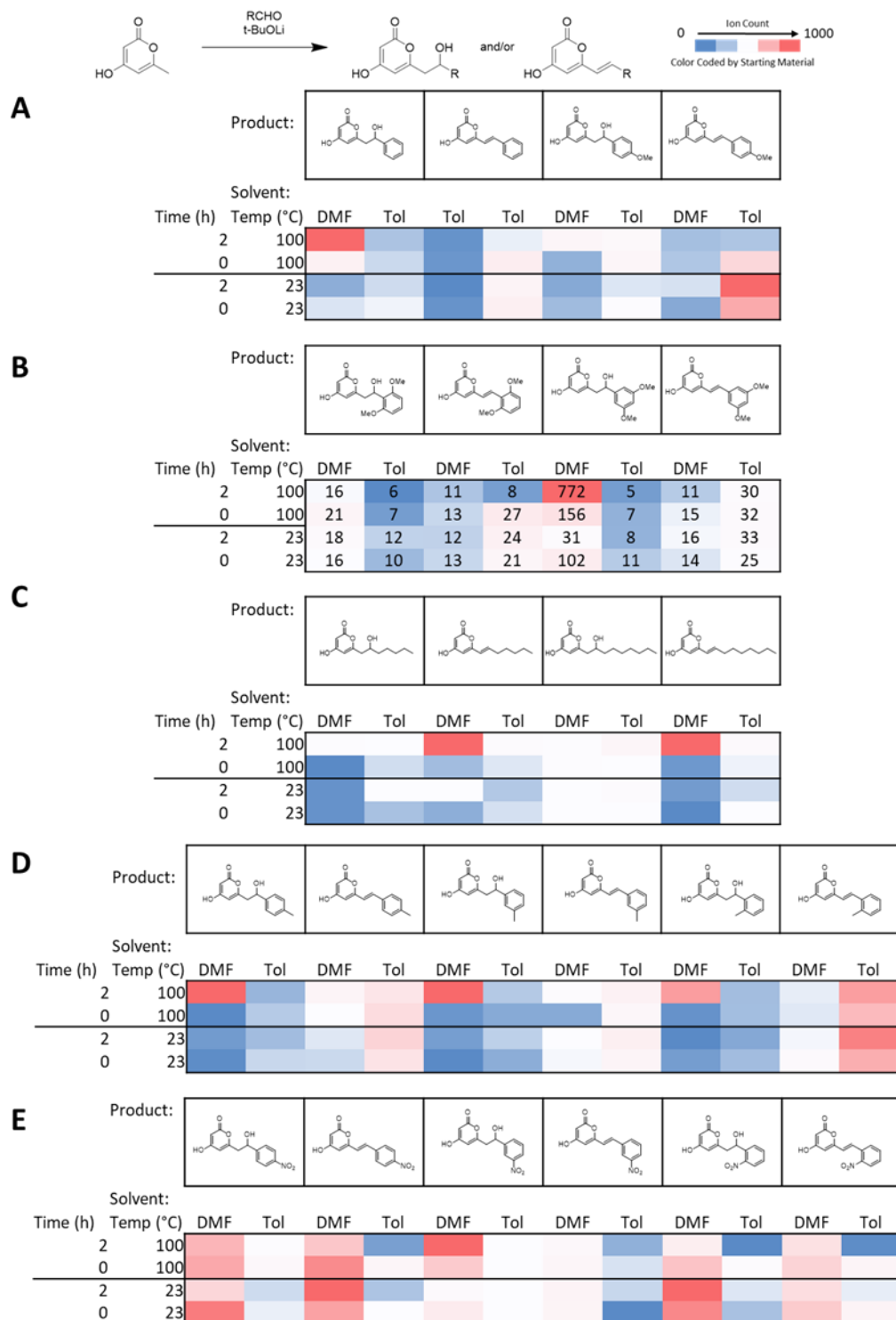


Figure 4.2. DESI-MS HTE heat map of the expanded aldol reaction set. Each cell is an average of 8 replicate reactions with normalized MS intensities. Heat maps are color coded by starting material type along the dark vertical lines in the tables. Ion intensity values are shown in the third heat map to more explicitly show the difference in substrate-based reactivity.

The most readily apparent trend is the consistent success of reactions carried out in DMF. Further, most of these reactions in DMF were more successful with the application of heat (Figure 2 A-E). Notably, the 2,6-dimethoxybenzaldehyde precursor gave lower conversion than the 3,5-dimethoxybenzaldehyde starting material, indicating that differences in reactivity based on steric factors may be detected with this method.

4.2.3 Microfluidic Validation

In order to validate the results of the DESI-MS experiment and build confidence in the capacity of these HTE experiments to predict upscaled reaction outcomes, several of the reactions were conducted under continuous flow conditions in a microfluidic reactor. A Chemtrix S1 system fitted with a 19.5 μL glass reactor chip with staggered-oriented-ridge (SOR) in line mixers (Figure 3) was used for this experiment. A solution of premixed 0.1 M TAL and 0.2 M lithium *t*-butoxide in DMF was flowed into one inlet to engage a 0.1 M aldehyde solution. A subset of the aldehydes evaluated in the DESI-MS HTE experiment were selected, specifically 4-methoxybenzaldehyde, hexanal, 2,6-dimethoxybenzaldehyde, and 3,5-dimethoxybenzaldehyde. Residence times of 0.5, 1, 2, 5 and 10 minutes and temperatures of 23, 100, and 200 $^{\circ}\text{C}$ were investigated. After emerging from the reactor, each sample was diluted 1:1000 into ACN and cooled to -80 $^{\circ}\text{C}$ until analysis by electrospray ionization MS (ESI-MS).

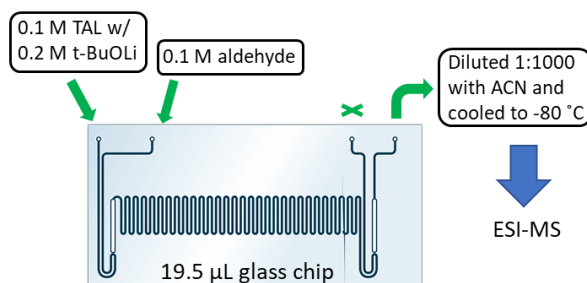


Figure 4.3. Microfluidic reactor schematic.

The aldehydes tested in the flow reaction screen each showed at least one condition that generated a product m/z by ESI-MS analysis. For further confirmation of product identity, MS/MS spectra were acquired for the product peaks and compared to the MS/MS of TAL (Figure 4) that showed a distinctive fragment at m/z 81.

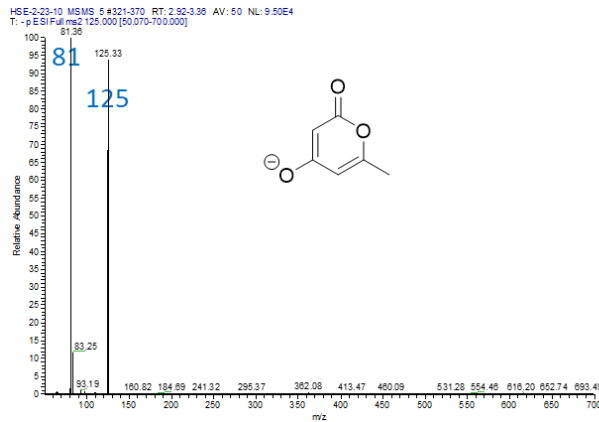


Figure 4.4. MS/MS spectrum of TAL.

For 4-methoxybenzaldehyde, the strongest product signal detected from the flow reaction screen was observed with a 2 minute residence time at a temperature of 23 °C. The peak at m/z 261 corresponds to the M-H peak in the negative MS mode, (Figure 5). MS/MS of this m/z 261 product gave a fragment at m/z 81, suggesting a structural similarity to TAL. There was, however, no evidence of the alcohol product, a finding consistent with the DESI result that showed easy formation of the elimination product of hexanal but no evidence of the alcohol product. The hexanal reactions showed evidence of the elimination product at m/z 207, but not of the aldol product. The greatest yield of the elimination product of hexanal and TAL was observed at a residence time of 10 minutes at 100 °C. This was the only case where the elimination product was observed in the set of microfluidic experiments. MS/MS analysis of the m/z 207 product revealed fragments at m/z 125 and m/z 81, suggesting that the m/z 207 species is the elimination product

of the aldol formed by the reaction of hexanal and TAL. Peaks at m/z 273 were observed in the aldol reactions of both 2,6- and 3,5-dimethoxybenzaldehyde, indicating the formation of the aldol adduct. Both had the highest product conversion at 2 minute residence times at 100 °C. Further, the MS/MS data for both the dimethoxy benzaldehyde substrates displayed fragments at m/z 125 and m/z 81. Counterintuitively, 2,6-dimethoxybenzaldehyde had a slightly higher conversion to the alcohol product than 3,5-dimethoxybenzaldehyde, however, the difference in the flow reaction outcomes were less marked than in DESI-MS HTE.

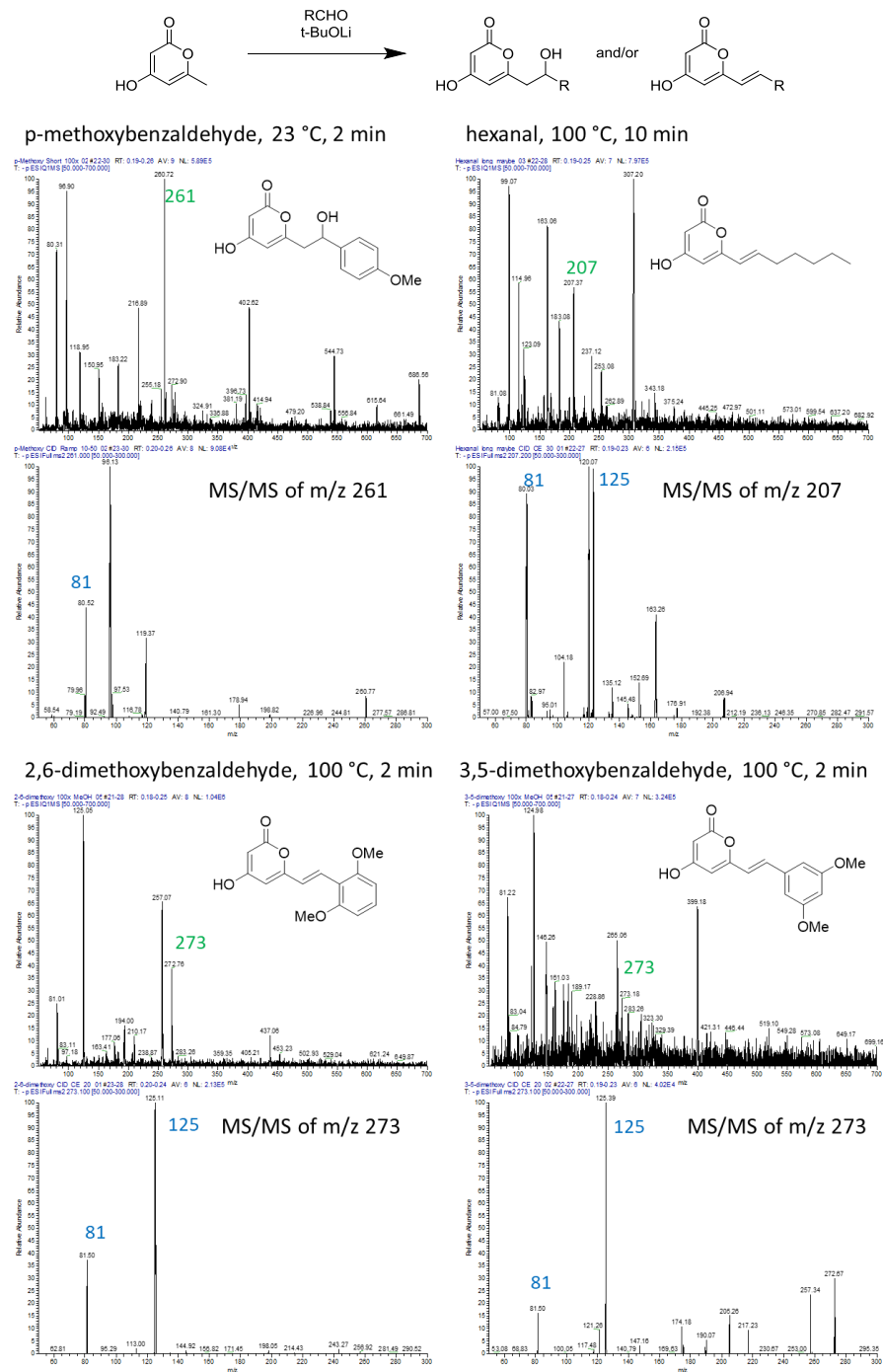


Figure 4.5. MS and MS/MS analysis of microfluidic reactions corresponding to DESI-MS HTE results.

4.3 Conclusions

We have demonstrated the use of DESI-MS analysis as an HTE tool. Using robotically prepared surface arrays of aldol reactions, the DESI-MS experiments were validated by corresponding microfluidic reactions analyzed by ESI-MS and MS/MS, to rapidly identify aldol derivatives of TAL. DESI-MS HTE showed hits for all aldehyde substrates tested and provided useful information to guide reaction scale up by continuous flow reaction with respect to solvent and temperature reactivity trends. This technology represents an opportunity to accelerate the process of platform chemical transformation so that bio-renewable replacements as well as novel chemical building blocks may be more quickly developed.

4.4 Future Directions

In addition to aldol reactions, several other classes of reactions have been carried out with TAL including amination, acylation, and others offering access to a variety of industrial and agrochemical products, active pharmaceutical ingredients, and chemical building blocks. In addition to HTE experiments with aldol reactions, a preliminary set of DESI-MS HTE experiments were carried out for amination and acylation reactions. Based on these preliminary results, these two reaction classes may be an interesting area for future exploration with DESI-MS HTE.^{1,3,8}

4.4.1 TAL Acylation

Following the same DESI-MS HTE procedures described for the aldol reactions, acylation reactions were also evaluated. Similarly to the aldol experiment, this experiment included 81 unique reactions sampled at 2 time points and 4 replicates each, there are a total of 648 data points.

The heat map in figure 4.6 shows the findings of this screen. The aliphatic acids hexanoic acid and 4-methylpentanoic acid showed particularly good conversion in toluene while benzoic acid showed poor conversion in toluene but better conversion in acetonitrile.

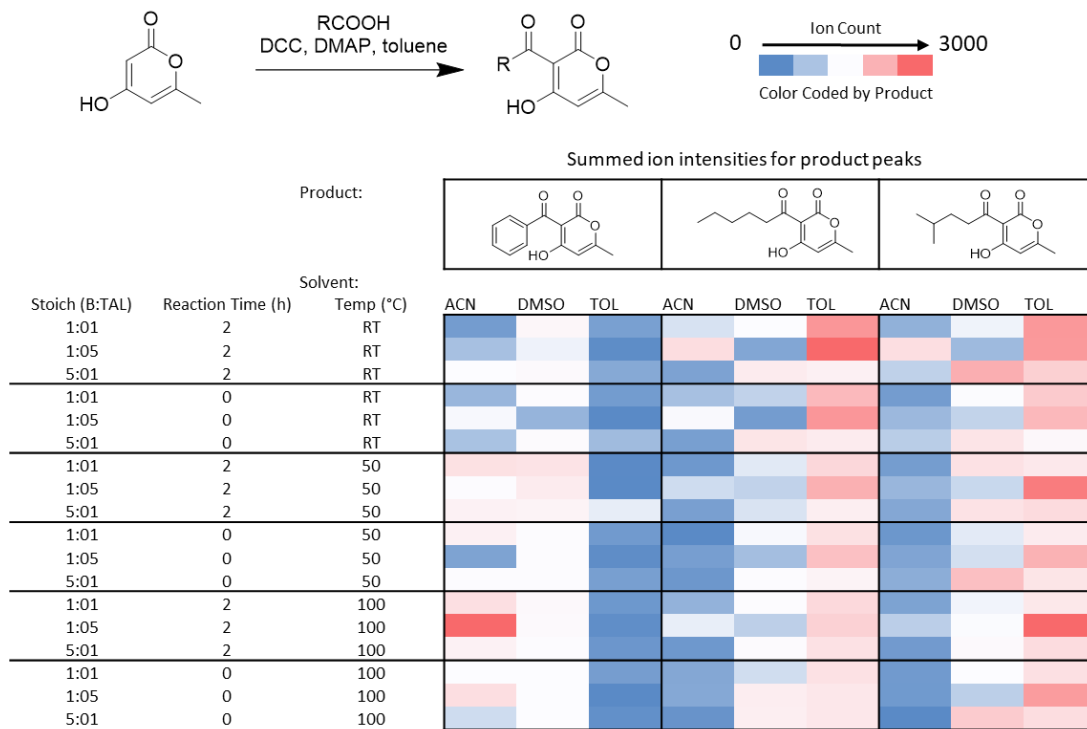


Figure 4.6. Heat map of acylation product signal intensities from aldol reactions of TAL with three substrates, three solvents, three stoichiometries and three temperatures. Each cell is an average of 4 replicates with normalized intensities. Heat maps color coded by product along the dark vertical lines.

4.4.2 TAL Amination

Amination reactions were explored next. Once again, this experiment included 81 unique reactions sampled at 2 time points and 4 replicates each, there are a total of 648 data points. Figure 4.7 summarizes the findings of this screen. The three amine substrates tested, benzylamine, p-bromoaniline, and cyclohexyl amine each showed hits at the product m/z when heated for two hours in water.

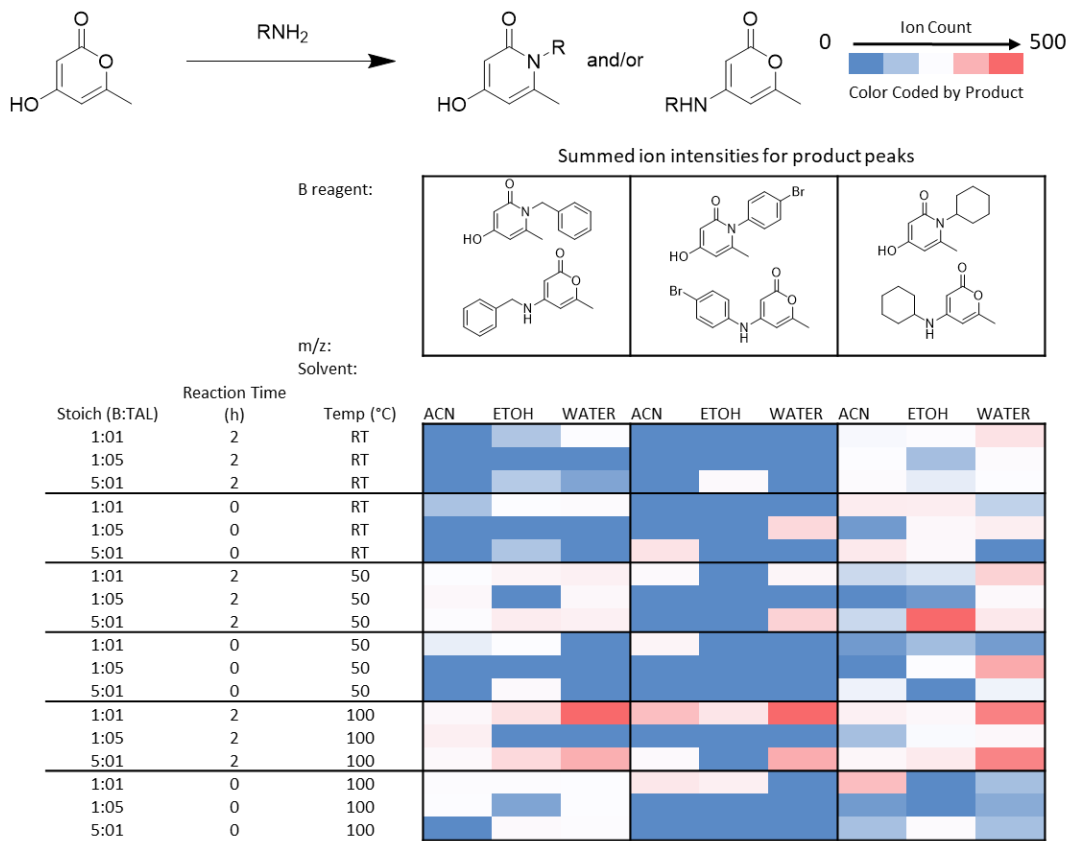


Figure 4.7. Heat map of amination product signal intensities from aldol reactions of TAL with three substrates, three solvents, three stoichiometries and three temperatures. Each cell is an average of 4 replicates with normalized intensities. Heat maps color coded by product along the dark vertical lines.

4.4.3 Outlook for DESI-MS HTE of Platform Molecules

The reactions explored in this study provide a proof of concept for the use of DESI-MS HTE to develop platform chemicals like TAL. TAL is only one among many possible molecules to explore using this technique. Other similar pyrones may be used in the same way to achieve alternative chemical building blocks with differing structural characteristics to TAL to diversify the range of accessible materials. Further, the polyketide branch of natural products of which TAL is a member offers a broad range of carbon chain lengths, offering a promising pool for platform chemicals.^{1,3,8}

4.5 Materials & Methods

4.5.1 General Procedure for DESI-MS Experiments

The DESI-MS experiments were conducted in the manner previously described by Wleklinski and co-workers.¹⁹ A Biomek i7 liquid handling robot (Beckman Coulter) was used to distribute reaction mixtures into master well plates (either 96 or 384 well plates, depending on the scope of the experiment). For heated reactions, the liquid handling robot was used to distribute reaction mixtures into aluminum well plates fitted with glass vials (Analytical Sales & Services, Inc.). These heated master plates were prepared were sealed with a PFA film and two silicone rubber mats before heating. Each reaction vial was prepared at 50 mM and contained at least 300 μ L of reaction mixture. After allowing the plates to cool, the reaction mixtures were transferred to secondary plates to be printed onto surfaces. A magnetic pin tool (V&P Scientific, Inc.) was interfaced with pod1 of the liquid handling robot and used to transfer 50 nL volumes of reaction mixtures from the master well plate to the porous PTFE surface for DESI-MS. A commercial DESI source (Prosolia, Inc.) and a Thermo LTQ linear ion trap were utilized to execute the DESI-MS experiment. Experiments were conducted in positive-ion mode (m/z 50-500) with pure methanol as the spray solvent (2.5 μ L/min). Parameters for the mass spectrometer and speed of the DESI stage were optimized previously.¹⁹ In-house software was used to process the data and generate spreadsheets from which heat maps were prepared.

4.5.2 General Procedure for Continuous-Flow Experiments

All microfluidic reactions were carried out using a Chemtrix Labtrix S1 system equipped with 3227 glass reactor chips with a volume of 19.5 μ L. A solution of 0.05 M TAL and 0.1 M lithium *tert*-butoxide together, and another of 0.05 M aldehyde in DMF were prepared. Syringes

were loaded with each of these solutions and positioned on the first two inlets of the Chemtrix 3227 chip. The reactants were engaged with 1 min, 2min, 5 min and 10 min residence times at temperatures of 50, 100, 150, and 200 °C. Samples were collected and immediately diluted 1:1000 in ACN and stored at -80 °C prior to analysis.

4.5.3 General Procedure for ESI-MS Analysis

Mass spectral analysis was performed for each flow and batch reaction sample using a Thermo TSQ triple quadrupole mass spectrometer (Thermo Fisher Scientific) equipped with an autosampler and electrospray (ESI) ionization. Reaction samples were diluted 1:1000 into ACN upon collection and cooled to -80°C to quench the reactions before warming to room temperature immediately prior to analysis. The distance between the tip of the spray emitter and the ion transfer capillary to the MS was kept constant at ca. 1.5 cm. Experiments were performed using a Thermo-Fisher HESI-II probe and Ion Max ion source. A spray voltage of 3.5 kV was used for all analyses.

4.6 References

- [1] Bozell, J.J.; Petersen, G.R. *Green Chem.* **2010**, 12, 539-554
- [2] Werpy, T.; Peterson, G. *Top Value Added Chemicals from Biomass. Vol. I*, U.S. D.O.E., **2004**
- [3] Nikolau, B.J.; Perera M.A.D.N.; Brachova, L.; Shanks, B. *The Plant Journal*, **2008**, 54, 536–545
- [4] Ciriminna, R.; Palmisano, G.; Della Pina, C.; Rossi, M.; Pagliaro, M. *Tetrahedron Lett.* **2006**, 47, 6993-6995
- [5] Pagliaro, M.; Ciriminna, R.; Kimura, H.; Rossi, M.; Pina Della, C. *Angew. Chem., Int. Ed.*, **2007**, 46, 4434–4440
- [6] Wang, T.; Nolte, M. W.; Shanks, B. H. *Green Chem.*, **2014**, 16, 548-572
- [7] Bicker, M.; Kaiser, D.; Ott, L.; Vogel, H. *Fluids*, **2005**, 36, 118-126

- [8] Keeling, P.L.; Shanks, B.H. *Green Chem.* **2017**, 19, 3177-3185
- [9] Xie, D.; Shao, Z.; Achkar, J.; Zha, W.; Frost, J.W.; Zhao, H. *Biotech. And Bioengineering,* **2006**, 93, 727-736
- [10] Chia, M.; Schwartz, T.J.; Shanks, B.H.; Dumesic J.A., *Green Chem.*, **2012**, 14, 1850
- [11] Kraus, G. A.; Basemann, K.; Guney, T. *Tetrahedron Lett.*, **2015**, 56, 3494-3496
- [12] Kraus, G. A.; Wanninayake, U. K.; Bottoms, J. *Tetrahedron Lett.*, **2016**, 57, 1293-1295
- [13] Kraus, G. A.; Wanninayake, U. K. *Tetrahedron Lett.*, **2015**, 56, 7112-7114
- [14] Mayr, L. M.; Bojanic, D. *Curr. Opin. Pharmacol.*, **2009**, 9, 580-588
- [15] Koehn, F. E., High impact technologies for natural products screening. In Natural Compounds as Drugs Volume I, Petersen, F.; Amstutz, R., Eds. Birkhäuser Basel: Basel, 2008; pp 175-210.
- [16] Janzen, W. P., *Chem. Biol.*, **2014**, 21, 1162-1170
- [17] Syahir, A.; Usui, K.; Tomizaki, K.; Kajikawa, K.; Mihara, H. *Microarrays*, **2015**, 4, 228-244
- [18] Wleklinski, M.; Falcone, C. E.; Loren, B. P.; Jaman, Z.; Iyer, K.; Ewan, H. S.; Hyun, S.; Thompson, D. H.; Cooks, R. G. *Eur. J. Org. Chem.* **2016**, 2016, 5480-5484.
- [19] Wleklinski, M.; Loren, B. P.; Ferreira, C. R.; Jaman, Z.; Avramova, L.; Sobreira, T. J. P.; Thompson, D. H.; Cooks, R. G. *Chem. Sci.* **2018**, 9, 1647-1653
- [20] Ewan, H. S.; Iyer, K.; Hyun, S.; Wleklinski, M.; Cooks, R. G.; Thompson, D. H. *Org. Process Res. Dev.*, **2017**, 21, 1566-1570
- [21] Loren, B. P.; Wleklinski, M.; Koswara, A.; Yammine, K.; Hu, Y.; Nagy, Z. K.; Thompson, D. H.; Cooks, R. G. *Chem. Sci.* **2017**, 8, 4363-4370
- [22] Falcone, C. E.; Jaman, Z.; Wleklinski, M.; Koswara, A.; Thompson, D. H.; Cooks, R. G. *Analyst*, **2017**, 142, 2836-2845
- [23] Cooks, R.G.; Ouyang, Z.; Takats, Z.; Wiseman, J.M. *Science*, **2006**, 311 , 1566-1570
- [24] Nemes, P.; Vertes, A. *Trends Anal. Chem.*, **2012**, 34 , 22 -34
- [25] Monge, M. E.; Harris, G.A.; Dwivedi, P.; Fernández, F.M. *Chem. Rev.*, **2013**, 113 , 2269 - 2308
- [26] Loren, B. P.; Ewan, H. S.; Avramova, L.; Ferreira C. R.; Sobreira, T. J. P.; Yammine, K.; Liao, H.; Cooks, R. G.; Thompson, D. H. *Sci. Rep.*, **2019**, 9,14745.

- [27] Adamo, A.; Beingessner, R. L.; Behnam, M.; Chen, J.; Jamison, T. F.; Jensen, K. F.; Monbaliu, J. M.; Myerson, A. S.; Revalor, E. M.; Snead, D. R.; Stelzer, T.; Weeranoppanant, N.; Wong, S. Y.; Zhang, P. *Science*, **2016**, 352, 61-67
- [28] Baumann, M.; Baxendale, I. R. *Beilstein J. Org. Chem.*, **2015**, 11, 1194-1219
- [29] Malet-Sanz, L.; Susanne, F. *J. Med. Chem.*, **2012**, 55, 4062-4098